UNIVERSITY OF GOTHENBURG

SAHLGRENSKA ACADEMY

EVALUATION OF RADIATION DOSES USING CONE BEAM COMPUTED TOMOGRAPHY IN ENDOVASCULAR AORTIC REPAIR AND SCOLIOSIS PROCEDURES

Louise Strandberg

Essay/Thesis:	30 hp
Program and/or course:	Medical Physics
Level:	Second Cycle
Semester/year:	Autumn 2018
Supervisors:	Pernilla Jonasson and Maria Larsson
Examiner:	Magnus Båth

Abstract

Essay/Thesis:	30 hp
Program and/or course:	Medical Physics
Level:	Second Cycle
Semester/year:	Autumn 2018
Supervisor:	Pernilla Jonasson and Maria Larsson
Examiner:	Magnus Båth
Keyword:	Cone beam CT, CT, EVAR, scoliosis, radiation dose, effective dose

---

Purpose: The study includes the two areas, vascular surgery and orthopedics, and focuses on endovascular aortic aneurysm repair (EVAR) and scoliosis procedures. EVAR procedures contribute to a high radiation dose to the patient and for scoliosis procedures, it is often young girls that are undergoing surgery. It is therefore important to keep the radiation doses as low as possible. The aim of this project was to evaluate the radiation dose when cone beam CT (CBCT) is used in interventional fluoroscopy and operating rooms (OR), for protocols used in EVAR and scoliosis procedures, ahead of optimization.

Theory: Ionizing radiation may be an important tool during surgery, for instance, to guide instruments through the patient blood vessels. In interventional fluoroscopy and angiography, two-dimensional (2D) imaging is widely used. However, to avoid overlay of the patient anatomy and improve visualization a CBCT can be performed, which gives a three-dimensional (3D) image of the patient. CBCT uses a cone beam shaped radiation field and can be performed during surgery using the interventional x-ray equipment. One advantage with this method is that a 3D image of the patient can be received without having to move the patient to a computed tomography (CT) room. CBCT and CT are imaging methods that give a relatively high radiation dose, which makes it important to evaluate differences between the two modalities.

Method: Two phantoms were used to evaluate the radiation doses, a polymethyl methacrylate (PMMA) phantom and an abdominal phantom. Dose area product (DAP), absorbed dose rate and incident air kerma (IAK) in the reference point (skin dose received from DICOM data) were collected for different protocols and settings on three modalities, *Artis Q*, *Pheno* and *Zeego*. Effective dose and absorbed organ doses were also calculated using PCXMC20Rotation. Image quality was evaluated using the high-resolution module in Catphan and the number of line pairs per cm was calculated. CT scans were performed and effective doses and equivalent doses were calculated using CT-Expo. 2D-fluoroscopy and exposure were performed with the abdominal phantom to evaluate DAP at 2D-3D-fusion. Personnel radiation dose was estimated using the real-time personal radiation dosimetry system, Dose Aware. Measurements were made at different distances from the patient center, on all modalities and for all protocols. Also, measurements with thermoluminescent dosimeters (TLD) was performed on both phantoms for one modality, *Artis Q*.

Result: The maximum difference, comparing the protocols giving the highest and lowest effective doses, was a factor of 16. Using collimation and zoom decreases the effective dose compared to the default setting. However, IAK in the reference point increased with both collimation and zoom. The quotient of effective dose for the scoliosis

protocols, for the normal dose protocols compared to the low dose protocols, was a factor 1.3 and 1.8, on *Artis Pheno* and *Artis Zeego*, respectively. For the two high radiation dose protocols used for EVAR procedures, on all modalities, CBCT gave a higher effective dose than CT, when using the same scan range. The two low radiation dose CBCT protocols, used for EVAR, gave a lower effective dose than the CT protocol with the same scan range. The CBCT protocols for scoliosis, on both modalities *Artis Pheno* and *Artis Zeego*, gave a higher effective dose than the CT scan using the same scan range, except for the protocols, *4sRygg Low dose 3D* and *CT Low dose 4s R15P85*, compared to the CT protocol *Full back (automatic).* Evaluating the high-resolution image quality on all protocols, for both EVAR and scoliosis, gave 8-9 lp/cm, except for the scoliosis protocol *CT Low dose 4s R15P85* on *Artis Zeego* which had a decreased resolution with 4 lp/cm. With 2D-3D-fusion a factor 10 lower DAP was received, when comparing six seconds fluoroscopy with the lowest dose protocol, *FL Low*, with the CBCT protocol *5sDR Body Care* on *Artis Q*. Using an increased distance to the patient, and settings such as collimation and zoom, decreased the estimated personnel radiation dose.

Populärvetenskaplig sammanfattning

Joniserande strålning är ett verktyg som kan användas vid både undersökning och behandling av patienter. Intervention är en metod som använder röntgenstrålning som vägledning för att behandla en patient. Med denna teknik används instrument, exempelvis en kateter, som förs in i patientens blodkärl. Genom ett litet snitt i patientens hud kan katetern föras in i exempelvis höftartären. Intervention är ett säkert ingrepp som har en snabb återhämningstid och kan användas för att behandla flera typer av sjukdomar. Med ballongsprängning (PCI) kan förträningar av hjärtats kranskärl behandlas. Denna metod använder en ballongkateter som förs in i blodkärlet, varpå ballongen blåses upp i området där förträningen finns. Angiografi är, till skillnad från intervention, en metod som använder röntgenstrålning för att undersöka blodkärl. En kateter förs in i blodkärlet och, då undersökningsområdet är lokaliserat, injiceras kontrastvätska och en serie röntgenbilder tas.

För att förbättra synbarheten under intervention och angiografi kan olika tekniker användas. Bland annat är digital subtraktionsangiografi (DSA) en teknik som används för att reducera bakgrunden i bilderna så att blodkärlen syns tydligare. Däremot kommer det alltid finnas viss överlagring av anatomin då 2D-bilder tas. Genom att rotera röntgenröret runt patienten utförs en cone beam datortomografi (CBCT). Med en CBCT fås en 3D-bild av anatomin och överlagringar undviks med denna metod. Datortomografi (CT) är en metod som också ger en 3D-bild av patienten, och är väl använt inom diagnostik. Däremot kan inte en CT utföras i en operationssal till skillnad från en CBCT, men används ofta inför och efter operationer för att planera ingreppet och för uppföljning.

Både CBCT och CT ger en relativt hög stråldos till patienten och det är viktigt att utvärdera skillnaderna mellan de båda röntgenutrustningarna, vad gäller både stråldos och bildkvalitet. Däremot finns det inget självklart sätt att jämföra stråldoserna från de olika modaliteterna. Stråldosen till patienterna ska alltid vara så låg som är rimligt möjligt, enligt ALARA-principen, vilket ändå gör det viktigt att utvärdera stråldosen per rotation och skillnader i stråldos och bildkvalitet, mellan både olika protokoll och röntgenutrustningar, så som CBCT och CT.

Då CBCT används under operationer, är det även viktigt att personalen använder de strålskydd som finns tillgängliga. När röntgenröret roterar kring patienten kommer den spridda strålningen till personalen öka. Ett ökat avstånd till patienten bör tas och strålskyddsförkläde och strålskyddsskärmar ska användas för att minska den spridda strålningen till personalen.

I arbetet har stråldoser från olika CBCT protokoll vid EVAR- och skoliosprocedurer kartlagts. Effektiv dos vid olika protokoll och modaliteter har bestämts och jämförts med effektiv dos från CT. Även bildkvaliteten mellan de olika protokollen har utvärderats samt stråldosen till personal har undersökts. I resultatet framgår att skillnaden i effektiv dos mellan olika protokoll varierar kraftigt. Mellan protokollet som ger högst stråldos och det som ger lägst skiljer det en faktor 16. Skillnaden i effektiv dos mellan CBCT och CT varierar kraftigt mellan olika protokoll. För CBCT protokollen som ger högst effektiv dos, ger dessa en högre effektiv dos än CT protokollen och omvänt för lågdos CBCT protokollen, då samma scanområde används. Den spatiella upplösningen mellan olika CBCT protokoll varierar ej. För att minska stråldosen till personalen bör ett ökat avstånd till patienten tas.

Table of content

Abbreviations

2D	Two-dimensional
3D	Three-dimensional
ALARA	As low as reasonably achievable
CBCT	Cone beam computed tomography
CT	Computed tomography
CTDI	Computed tomography dose index
$CTDI_w$	Computed tomography dose index weighted
$CTDI_{vol}$	Computed tomography dose index volume
DAP	Dose area product
DICOM	Digital Imaging and Communications in Medicine
DLP	Dose length product
DSA	Digital subtraction angiography
EVAR	Endovascular aortic aneurysm repair
FDD	Focus-to-detector distance
FRD	Focus-to-reference distance
IAK	Incident air kerma
MDCT	Multi-detector computed tomography
OR	Operating room
PCI	Percutaneous coronary intervention
PCXMC	PC-program for X-ray Monte Carlo
PMMA	Polymethyl methacrylate
ROI	Region of interest
TLD	Thermoluminescent dosimeter
VOI	Volume of interest

1 Introduction

During image-guided procedures, ionizing radiation is an important tool. Image-guided procedures are used in many different areas for both examination and treatment of patients. The equipment used for image-guided surgeries with x-rays are becoming more available and therefore, the use of these techniques are increasing. Image-guided surgery with x-rays can be used to, for instance, visualize and in real time guide instruments through the blood vessels. Interventional fluoroscopy is a method that uses image-guided surgery with x-rays for treatment of disease. With this technique instruments, such as catheters, is guided through the patient blood vessels. For instance, by making only a very small nick in the patient's skin the catheter is inserted through the femoral artery. This makes it a minimally invasive method with a short recovery time [1, 2]. Several types of diseases can be treated by using interventional fluoroscopy methods. For instance, narrowing of the coronary arteries can be treated by percutaneous coronary intervention (PCI). PCI is a procedure that uses a catheter, often a balloon catheter, to enter the blood vessel. During the procedure, x-ray imaging is used which enables visualization of the vessels in real time. When the damaged area is located the balloon is inflated to relieve narrowing of the coronary artery [3]. Like interventional fluoroscopy, angiography is a technique that also uses x-rays for image-guided surgery, however, instead, it is used to diagnose a disease. A catheter is inserted and when the examination area is located a contrast agent is injected and a series of x-ray images is taken [4].

To enhance visualization when using interventional fluoroscopy and angiography different techniques can be used. By rotating the x-ray equipment around the patient, a cone beam computed tomography (CBCT) is achieved. Many projection images around the patient are collected, often in a limited angular interval [5], and the data is reconstructed into CT-like images [6, 7]. This technique gives a 3D image of the anatomy, instead of a 2D image, which improves the visibility of the anatomical structures and avoids overlay.

The x-ray equipment, in interventional fluoroscopy and angiography, is used for visualization during minimally invasive procedures. Computed tomography (CT) is used for diagnostics and also provides a 3D image of the patient. The CT is used for planning the procedure and for follow-up. A CT is performed in the same way as CBCT, but the imaging methods differ slightly. CBCT uses a cone beam geometry and the CT a fan beam geometry. Also, a CT is not normally placed in an operating room (OR) unlike CBCT modalities, which makes it more difficult to use during surgery. However, CT imaging is still often used before surgery to, for example, enable the surgeon to plan the surgery. Both CT and CBCT are imaging methods that give a relatively high radiation dose to the patient. Often surgeons have good knowledge of radiation doses to patients undergoing a CT. This results in CT being an appropriate modality to compare the radiation doses received from CBCT. However, one difficulty with the two imaging methods is how to compare the radiation dose to the patient, which is not quite intuitive since the modalities measure different radiation dose quantities. The radiation dose received by the patients should always be treated according to the "as low as reasonably achievable" (ALARA) principle, which makes it important to evaluate the differences between the two modalities.

The introduction of CBCT into the OR room has made a big difference in how the examination and treatment are performed. For example, a complete rotation of the examined area can be performed during surgery, in the same room. However, the scattered radiation to the personnel increases with the rotations compared to 2D imaging. During a CT scan, the personnel is normally not inside the examination room unlike during a CBCT in an OR. It is therefore very important that the personnel uses radiation protection such as radiation protection aprons, radiation shields and additional distance to the patient, to avoid scattered radiation during CBCT. Also, since the equipment using image-guided surgery with x-rays are becoming more accessible it is important to evaluate the radiation doses, especially from CBCT, since these radiation doses might be high, compared to 2D imaging.

Two procedures that use CBCT is Endovascular aortic repair (EVAR) and scoliosis. In EVAR procedures the radiation doses to patients are high due to long fluoroscopy times and 2D imaging. Also, sometimes CBCT is used in more complex cases when the patient has a curvature of the aorta, for example. In scoliosis procedures the only x-ray imagining used is CBCT, to makes sure that the pedicle screws does not harm any risk tissue. The radiation doses during a scoliosis surgery are therefore significantly lower compared to EVAR. However, the scoliosis procedures are often performed on young girls and these patients go through several examinations with x-rays, both to diagnose the scoliosis and for follow-up.

The overall aim of this project was to survey the radiation doses using CBCT, for future optimization efforts. This included verification of dose differences between protocols and modalities, and investigation of the image quality when CBCT imaging is used in interventional fluoroscopy and OR. The work included the two areas of vascular surgery and orthopedics, with the focus on EVAR and scoliosis procedures. The radiation dose quantities, for the CBCT protocols, evaluated were; dose area product (DAP), DAP per detector area, absorbed dose rate, incident air kerma (IAK) in the reference point, effective dose and absorbed organ doses for skin, active bone marrow, colon, kidneys, ovaries and small intestine. Image quality for different protocols on different modalities were evaluated and compared. The calculated effective dose from CBCT was compared with the effective dose received from a CT examination. Also, the DAP received when performing 2D-3D fusion were compared with 3D-3D-fusion. Finally, the personnel radiation dose, in $H_p(10)$, was estimated during CBCT at different distances from the patient.

2 Background

2.1 Sahlgrenska University Hospital

2.1.1 Vascular Surgery

In the department of abdominal radiology both examinations and therapies which include the abdominal organs and vessels are performed. During surgery, x-ray is used to visualize the instruments, such as catheters, which helps the surgeon to guide through the vessels in real time. Endovascular aortic aneurysm repair (EVAR) is one of many treatments performed. The word, aneurysm, means dilatation, and the procedure is made to remove the risk of rupture of the aneurysm [8]. Most common is an abdominal aortic aneurysm [9]. Before the surgery, a diagnostic CT is performed for planning the EVAR procedure so that the stent grafts are placed correctly and do not obstruct the renal artery. With fusion, this plan can be seen during the surgery, as an overlay of another data set received at the surgery [9] (see section 2.6). During the procedure, a stent graft is implanted in the aorta while guiding the instruments through the femoral arteries with the help of x-ray. Series of x-ray images (exposures) are taken at several times during surgery, to confirm, for instance, the position of the renal arteries. During some surgeries, a CBCT can be performed to receive a 3D image of the treated area and at the end of the surgery, a CBCT can be achieved to ensure that the stent is correctly placed. Also, approximately one month after the surgery, a CT is performed to make sure there is no leakage in the operated area and that there is no risk of leakage in the future.

2.1.2 Orthopedics

In the department of Orthopedics, x-ray is used as visual guidance during surgery. In this department, the surgeries can, for instance, be performed in a hybrid OR, where the imaging device is incorporated in the OR [1]. One of the many conditions treated in the orthopedics department is scoliosis, which is a condition where the spine has a sideway curve. The incidence of scoliosis is the same between females and males. However, the risk of progression of the vertebral derotation is more common for females [10, 11]. A vertebra derotation of more than 30° is five times higher for females than for males [12]. To diagnose scoliosis, and for follow-up, a 2D x-ray, lateral and frontal, is usually performed [13]. If the degree of the vertebral derotation becomes bigger than 45° surgery is needed [12]. Before surgery, the patient is examined with a low-dose CT. This entails that the surgeon beforehand can plan the surgery, choose the appropriate size of screw and how to place them correctly [11]. During surgery, the surgeon places the pedicle screws in the patient's vertebrae and when all screws are in place a CBCT with the x-ray equipment in the OR is made. The CBCT gives a 3D image of the spine and pedicle screws. It is made to ensure that the pedicle screws are placed correctly and do not harm any risk tissue, such as the aorta or spinal cord. Finally, rods are placed in the pedicle screws to align the spine.

2.2 Computed tomography

Computed tomography, also called fan beam CT, is a method that produces a 3D image by using a fan beam. In the process of receiving a CT image, the x-ray tube and detector row are rotated around the patient [14], as shown in Figure 2.1. By moving the patient table during exposure, a larger area of the body can be imaged. The detectors measures x-ray transmission in a large number of projections around the patient, normally in a 360° angle interval. The transmission profiles are used in the reconstruction to obtained CT images [6]. The most common reconstruction methods are iterative reconstruction and back projection [14]. CT imaging is fast and can be used over the whole body. It is also used in diagnostics and patient follow-up. The radiation dose received from a CT is normally given as computed tomography dose index volume ($CTDI_{vol}$) and dose length product (DLP), see sections 2.8.4 and 2.8.5, respectively.

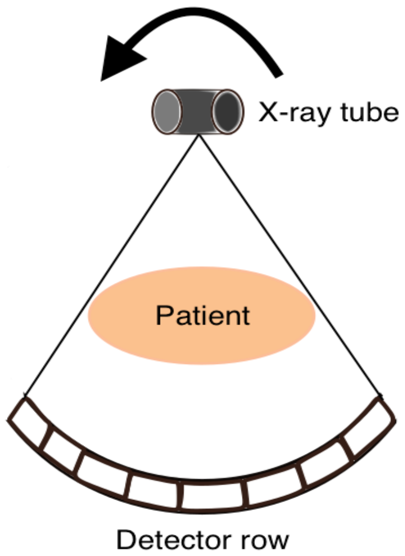

Figure 2.1: The geometry of the CT (single slice). The x-ray tube and detector row rotate around the patient.

The use of CT imaging has rapidly increased, and also the CT scanners have developed. Multi-detector CT (MDCT) scanners are nowadays used, in several sizes, and collimation widths are still increasing. With MDCT the scan time is decreased, however, the estimation of radiation dose has become a larger concern. $CTDI_{100}$ (section 2.8.4) is a quantity used to calculate the radiation dose in a CT scan. In all CT scans the dose profile will result in a tail perpendicular to the cross-section, which arises from the leakage and scattered radiation [14]. With larger collimation widths the tail becomes longer, because of the contribution of radiation dose from nearby slices [14, 15]. With longer tails, the pencil chamber, used for the measurements, does no longer collect all of the tail signal, which causes trouble with the quantity $CTDI_{100}$ [16]. When using larger collimation widths the fan beam CT approaches a cone beam CT (CBCT).

2.3 Cone beam CT

A CBCT is performed when an x-ray modality with a cone beam geometry rotates around the patient. In Figure 2.2 the cone beam geometry is demonstrated with the associated x-ray tube and image detector. CBCT is often used in dental imaging, but can also be performed in interventional radiology and orthopedics with, for instance, fluoroscopic systems, such as c-arms [6]. CBCT is used as an adjunct method and the purpose is to improve visualization and avoid overlay of the anatomy [6]. When performing a CBCT 2D data are collected in many projections, as the equipment is rotated around the patient, normally with a 200° angle interval. [5]. The data are thereafter reconstructed into CT-like images [7], often using filtered back projection. The radiation dose from a CBCT is given in dose area product (DAP), see section 2.8.3.

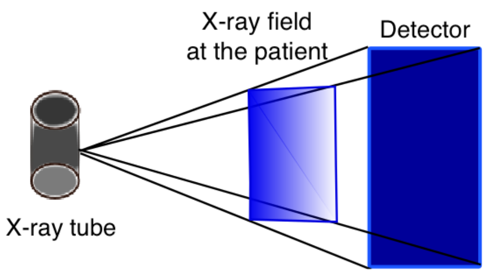

Figure 2.2: The geometry of a cone beam with an x-ray tube, x-ray field at the patient and detector.

2.4 CT vs CBCT

One difference between a conventional fan beam CT and a CBCT performed with fluoroscopic systems is that the CBCT rotation normally is performed in a limited angle, often 200° instead of 360° [5]. A CBCT can visualize the patient anatomy over a larger volume than a CT in one scan and also has a higher spatial resolution [17]. However, the CT is producing images with better low contrast in soft tissue and with a higher anatomical accuracy [17]. Shorter scan times are also one advantage for CT over CBCT, but with CBCT the imaging can be performed during surgery in the OR.

2.5 Digital subtraction angiography

To enhance visualization during image-guided procedures using x-ray several techniques can be used. With digital subtraction angiography (DSA), a two-dimensional (2D) image with reduced visual anatomical structures is achieved. An image without a contrast agent, a mask, is subtracted from an image with a contrast agent, which makes the vessels more visible [6, 18]. However, this does not always give the information needed. When studying intracranial aneurysms and during EVAR procedures a CBCT can be used [9, 19, 20]. During a procedure, both DSA and CBCT may be used in combination, 3D DSA, to improve visualization even further [18].

2.6 Fusion

To make surgeries safer and more accurate, techniques like fusion can be used. Before the surgery, the surgeon can plan the procedure based on CT images, and with fusion the plan can be seen during the surgery. With fusion an overlay of two datasets, or more, is seen on one screen [9]. These methods can also help reduce the radiation dose to the patient and personnel during surgery as the fluoroscopy times may decrease [21]. When performing fusion a preoperative CT image is imported to the workstation. In the next step either a 2D-3D or 3D-3D-registration can be made [7, 22]. With 2D-3D-registration two fluoroscopy images, one frontal and one lateral are taken and with 3D-3D-registration a CBCT is performed. These images are then merged with the preoperational CT. An algorithm is used to register the images to the same coordinate system and the result gives an image that lays as a mask over the real-time fluoroscopy image [7]. One advantage with 2D-3D-fusion over 3D-3D-fusion is the reduced radiation dose when using fluoroscopy images instead of performing a CBCT [9].

2.7 Thermoluminescent dosimeter

A thermoluminescent dosimeter (TL dosimeter or TLD) is a dosimeter that is commonly used to measure ionizing radiation. TLDs can be used for both patient and personnel monitoring [23]. Its small size, linear dose response and the fact that the TLD is reusable are some of the advantages. The TLD is made of a crystal, and by adding imperfections in the crystal lattice structure, energy levels in between the valence and conduction band of the crystal are created. When a TLD is irradiated, the electrons that gain enough energy will move from the valence band to the conduction band. Electrons in the conduction band will eventually lose their energy and move back to the valence band, while at the same time emitting light. However, some of these electrons, that do not lose enough energy, will get trapped in the energy levels created by the imperfections. By heating the crystal, the trapped electrons will move back to the conduction band and then to the valence band while emitting light. By collecting the light emitted, information about the received radiation dose is gathered [24]. This entails that TLDs are used for measurements of the integral dose, and not for instant results [23]. One type of TLD that can be used for health and dosimetry is DXT-RAD Ringlets TLD-100, *Thermo Scientific, USA*. This TLD has a crystal of the material lithium fluoride (LiF:Mg, Ti) and is suitable for photon and environmental measurements that are neutron free [25].

2.8 Dose quantities

2.8.1 Absorbed dose

Absorbed dose, D, is a quantity used for all types of ionizing radiation [26]. The definition of absorbed dose is given by Eq. (1),

$$D = \frac{d\bar{\varepsilon}}{dm} \quad (1)$$

where, $d\bar{\varepsilon}$, is the mean energy imparted [J] to matter by ionizing radiation and, dm, is the mass [kg]. The unit of absorbed dose is Gray [Gy] which is the same as joule per kilogram [J/kg] [26].

2.8.2 Effective dose

Effective dose, E, is a risk quantity calculated for a reference person where the weighting factors are an average of sex and age [26]. This quantity should not be used as a measure of risk for the individual person but can be used for a population. The effective dose is defined as Eq. (2),

$$E = \sum_{T} H_T \, w_T \quad (2)$$

Where, H_T, is the equivalent dose [J/kg] in a tissue or organ and, w_T, is the tissue weighting factor. The equivalent dose is defined as Eq. (3),

$$H_T = \sum_{R} D_{T,R} w_R \quad (3)$$

where, $D_{T,R}$, is the mean absorbed dose [J/kg] in a tissue, T, from radiation, R, and, w_R, is the radiation weighting factor [26]. The radiation weighting factor for photons (x-rays) is equal to one. The unit for both effective and equivalent dose is Sievert [Sv], which is the same as joule per kilogram [J/kg].

2.8.3 Dose Area Product

The dose area product, DAP, is the integral of absorbed dose over the radiation field area [6], Eq. (4),

$$DAP = \int D(x,y)dxdy \quad (4)$$

where, D(x,y), is the absorbed dose [Gy] in a point (x,y). The unit of DAP is [$Gycm^2$] but can be expressed with different prefixes. Since the absorbed dose decreases with the square of the distance, according to the inverse square law, and the irradiated area increases with the square of the area, the DAP remains the same regardless of the source-to-object distance [6].

2.8.4 Computed Tomography Dose Index

Several types of CTDI have been defined to describe the radiation dose from a CT scan. The absorbed dose in air, measured in a polymethylmethacrylate (PMMA) phantom, is defined as $CTDI_{100}$ [14], Eq. (5),

$$CTDI_{100} = \frac{1}{nT} \int_{-50}^{50} D(z)dz \quad (5)$$

where, D(z) [Gy], is the absorbed dose integrated over a length of 100 mm and, n, is the number of simultaneously acquired slices and, T, [mm] is the nominal slice thickness. Since the CT scan is performed over 360 degrees the expression CTDI weighted ($CTDI_w$) is defined to take into account the spatial variation of the absorbed dose [14]. $CTDI_w$ weights the absorbed dose in the peripheral positions higher than in the central position and is described as Eq. (6).

$$CTDI_w = \frac{1}{3} CTDI_{100,c} + \frac{2}{3} CTDI_{100,p} \quad (6)$$

$CTDI_{100,c}$, is the absorbed dose in the central position of the phantom measurement and, $CTDI_{100,p}$, is the averaged value from the peripheral measurements. The $CTDI_w$ does not account for the radiation dose received when a spiral scan is performed which result in CTDI volume, $CTDI_{vol}$ [14], Eq. (7),

$$CTDI_{vol} = \frac{CTDI_w}{pitch} \quad (7)$$

where the pitch is defined as the ratio of the table movement in one gantry rotation [mm] and the nominal collimation width. The unit of the CTDI is [Gy] and $CTDI_{vol}$ is the most common index used to express the radiation dose in a CT scan [14].

2.8.5 Dose Length Product

By taking the total scan length into account the dose length product (DLP) is introduced. This is defined as Eq. (8),

$$DLP = CTDI_{vol} \cdot l \quad (8)$$

where, l, is the total scan length. The unit for DLP is [Gym] [14].

2.8.6 $H_p(d)$

$H_p(d)$ is a personal dose equivalent and represents the dose equivalent at the depth of *d* mm in soft tissue. $H_p(d)$ is used to measure radiation doses to personnel from external radiation. $H_p(10)$, representing d = 10 mm, is used for the assessment of effective dose. $H_p(0.07)$ is used to assess the dose to skin and represents the depth d = 0.07 mm. $H_p(10)$ and $H_p(0.07)$ is often measured when performing individual monitoring on personnel working with radiation [26].

2.9 PCXMC20Rotation

For calculating effective doses from CBCT the Monte Carlo program, a Personal Computer (PC) program for X-ray Monte Carlo 20 Rotation (PCXMC20Rotation) [27], may be used. PCXMC20Rotation is a supplementary program to PCXMC [28] which allows calculations when the x-ray system rotates around a center point of rotation. PCXMC uses tissue weighting factors from both International Commission on Radiological Protection (ICRP) Publication 103 and 60 [26, 29], and phantom models of Christy and Eckerman (1987) describe the anatomical data [27]. The phantom models are hermaphrodites and some changes to the phantoms have been made to make them more realistic and enable calculations with the tissue weighting factors from ICRP 103 [27]. The effective dose and estimated absorbed organ doses for different examination conditions can be calculated and allows user-supplied input parameters to be used.

2.10 CT-Expo

CT-Expo v2.5 is a program used to calculate patient dose in CT-examinations. It is an Microsoft Excel application written in Visual Basic [30]. CT-Expo allows age- and sex-specific dose values and the scan range can be set individually. It also allows selection of scanner model (manufacturer and type of scanner) to perform more dedicated dose calculations. To perform the calculation the actual scan parameters are also needed as input. Several quantities can be calculated using CT-Expo, including $CTDI_{vol}$, DLP, effective dose and equivalent doses for organs. The effective doses can be calculated according to both ICRP Publication 103 and 60 [26, 29].

3 Methods and materials

3.1 Phantoms

One of the phantoms used in this study was an anthropomorphic abdominal phantom, see Figure 3.1, which represents a normal sized man. With this phantom absorbed dose using TLDs, DAP, DAP per detector area, IAK in the reference point (from *Digital Imaging and Communications in Medicine* (DICOM) data), absorbed dose rate, was determined and effective dose and absorbed organ doses was calculated. The phantom is made of PMMA and contains the skeleton parts, spine and pelvis, of the abdomen. The skeleton in the phantom is made of plastic. The phantom was always in a supine position, with the head in the head direction of the table. Measurements were made with the abdominal phantom placed on the table, both with and without TLDs. When TLDs were used they were evenly distributed on the surface, in a circle around the abdominal phantom, shown in Figure 3.2.

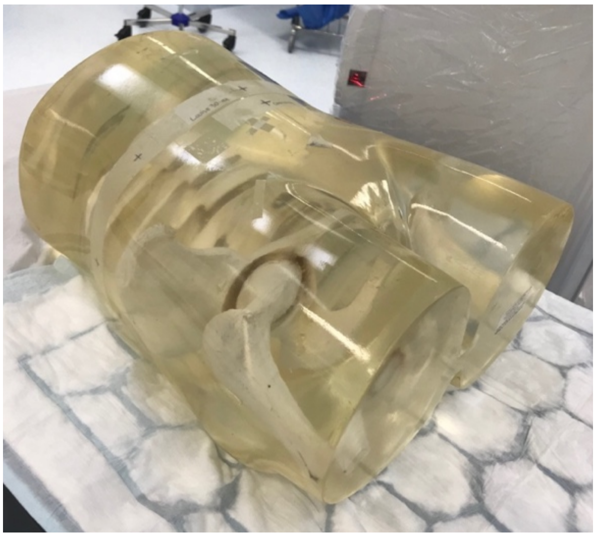

Figure 3.1: Abdominal phantom used for measurements.

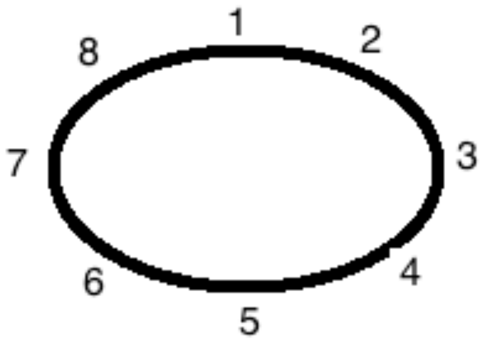

Figure 3.2: Distribution of TLD-100 on the abdominal phantom. TLD position 7 is on the right-hand side of the phantom and position 3 on the left. The rotation of the x-ray tube starts between the positions 7 and 8, and ends between positions 3 and 2.

Another phantom used, for TLD radiation dose measurements, was made of three PMMA blocks and five slices of PMMA, Figure 3.3. All of the blocks have handles and the dimensions are 5×25×30 cm^3. Above, underneath and between the blocks, the slices of PMMA were placed. The slices placed on the top and bottom have the dimensions 1×25×30 cm^3, and the slices in-between have the dimensions 0.2×25×30 cm^3. The total phantom size was 17.6×25×30 cm^3. Consideration of the handles has been taken in such a way that the x-ray beam was positioned centric over the homogeneous part of the phantom. The handles were placed on the head side of the table (yellow arrow), and the right and left side of the phantom was defined as the right and left-hand side of a patient lying in a supine position. The red arrow in Figure 3.3 shows the CBCT rotation.

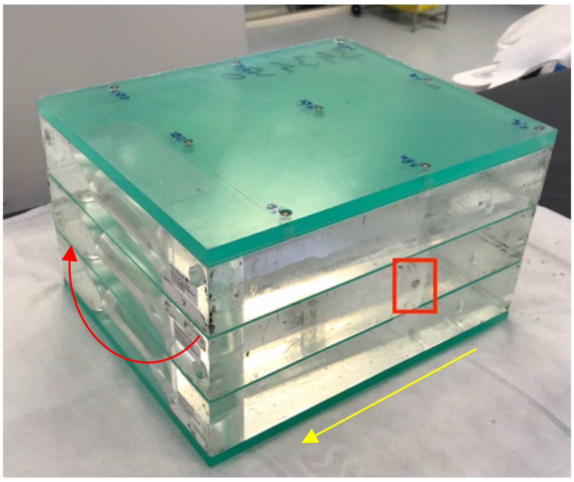

Figure 3.3: The PMMA phantom. The right side dosimeter is marked as red in the figure. The yellow arrow points at the head direction and the red arrow shows the CBCT rotation.

All of the PMMA-slices have holes in them (diameter 8 mm and depth 1 mm) in which the TL dosimeters were placed, Figure 3.4 and 3.5. The dosimeter positions have been numbered according to slice plane and TLD position. The depths of the TLD positions in the planes one to five were, 0.05, 1.05, 6.25, 11.45 and 16.65 cm, respectively, see Figure 3.4.

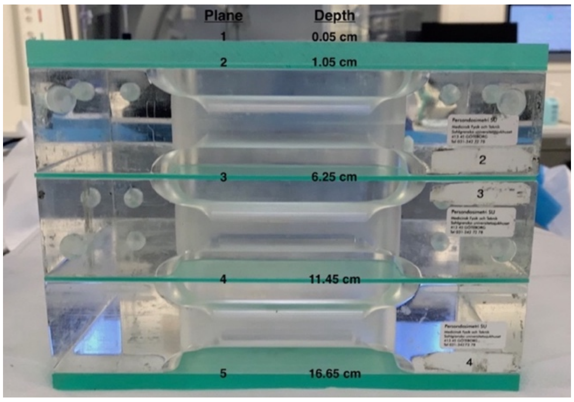

Figure 3.4: The PMMA phantom planes and its depths.

In each plane, there were nine dosimeter positions, all at different coordinates, and the numbering goes from the top left corner to the bottom right corner, as shown in Figure 3.5. For example, a dosimeter placed in plane 5 and position 6 was numbered 5.6.

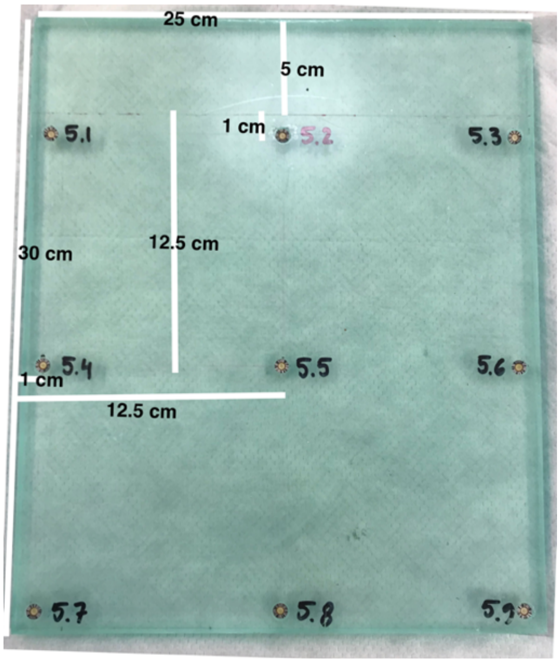

Figure 3.5: Numbering and coordinated of the dosimeters in the PMMA phantom.

Also, one dosimeter was placed in a small pocket in the center of the PMMA phantom, on the right and left-hand side, see the red marking shown in Figure 3.3.

To evaluate the image quality another phantom, *Catphan 600, The Phantom Laboratory, USA,* was used. The section used was CTP528, see Figure 3.6, which is a high-resolution module and contains 21 line pair per cm gauge and point source [31].

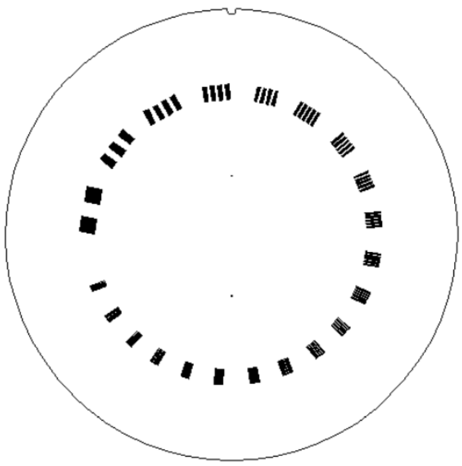

Figure 3.6: Section CTP528 in the phantom Catphan [31]. The section contains 21 lp/cm.

Three x-ray modalities were used for the CBCT measurements, *Artis Q*, *Pheno* and *Zeego, Siemens Healthineers, Germany*. The possible angular interval for CBCT acquisition, are different between the three modalities, but for the different protocols, EVAR and scoliosis protocols on each modality, the same angle interval of 200° was used. The angular interval for CBCT acquisition is presented in Figure 3.7, for all modalities and the EVAR and scoliosis CBCT protocols.

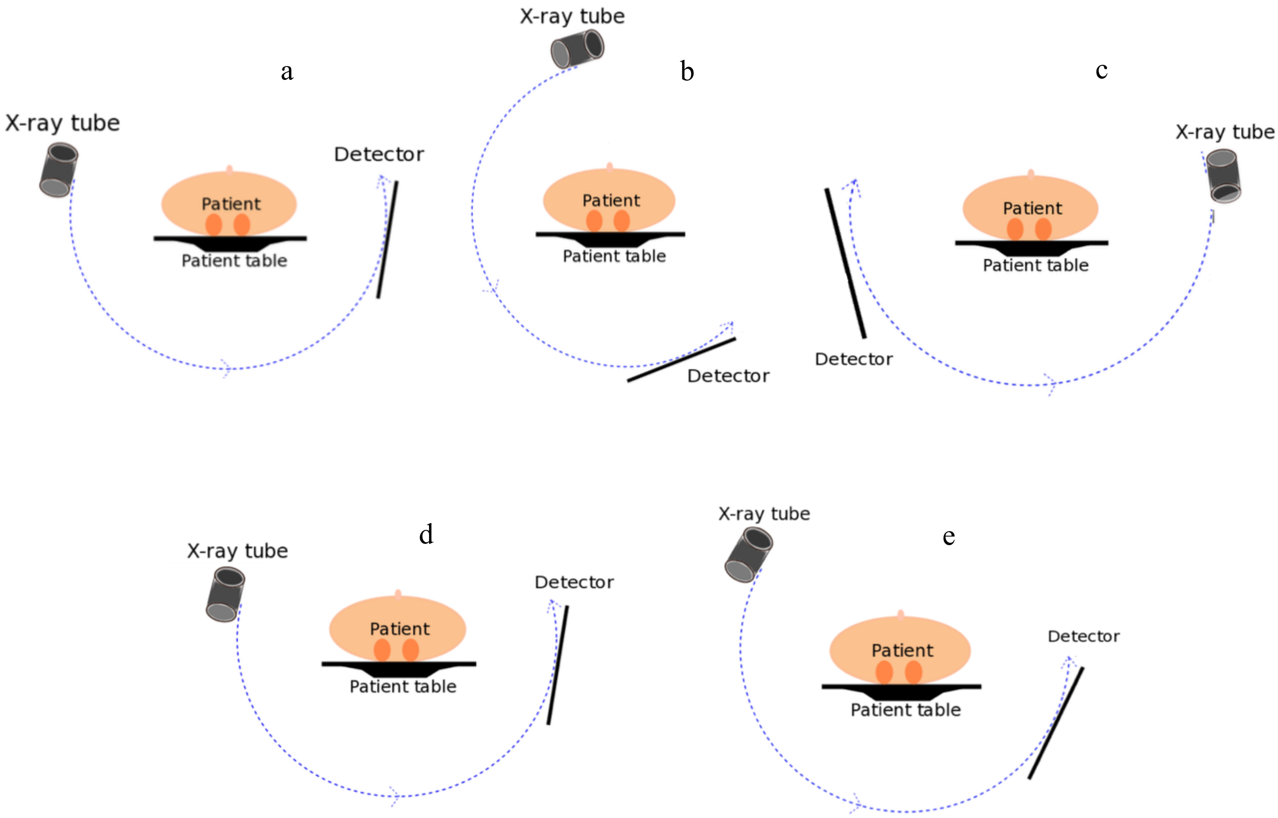

Figure 3.7: A schematic view of the angular interval for CBCT acquisition around the patient for the different modalities, for both EVAR and scoliosis. The figures represents the CBCT rotation for EVAR protocols on a: Artis Q, b: Artis Pheno, c: Artis Zeego, for scoliosis protocols on d: Artis Pheno and e: on Artis Zeego. All protocols were rotated with the angle interval of 200°.

3.2 Protocol Comparison

3.2.1 Radiation dose

The radiation dose for different protocols, used for EVAR and scoliosis, on three different modalities was evaluated. The radiation dose quantities evaluated were; DAP, DAP per detector area, absorbed dose rate, IAK in the reference point (DICOM data), effective dose and absorbed organ doses. Effective dose and absorbed organ doses were calculated from exposure parameters using PCXMC20Rotation, see section 3.7.1. For all measurements, the mattress was placed on the table.

The radiation dose received by one CBCT rotation, for different protocols on the different modalities, *Artis Q*, *Pheno* and *Zeego*, were compared. The abdominal phantom was used and centered in the same way on all modalities, using markers on the phantom. Four EVAR protocols, group 1, 2, 3 and 4, were compared on all three modalities and two scoliosis protocols were compared, only on *Artis Pheno* and *Artis Zeego*. The groups of protocols used on each modality are presented in Table 3.1, each row in the table are representative in radiation dose. The protocols for EVAR on *Artis Q* and *Artis Pheno* were found under the heading *3D Body* and on *Artis Zeego* under *InSpace3D Body R30* and *Dyna CT Body R30*. The protocols for scoliosis were found under the heading *Orthopedics* and *3D Rygg R15P85* on *Artis Pheno* and *Artis Zeego*, respectively.

Table 3.1: CBCT protocols compared on the modalities Artis Q, Artis Pheno and Artis Zeego, for EVAR and scoliosis.

	Modality			
	Artis Q	**Artis Pheno**	**Artis Zeego**	
EVAR	6sDCT Body	5sDCT Body L	8sDCT Body R30	Group 1
	5sDCT Body Care	4sDCT Body Care L	5sDCT Body Care R30	Group 2
	5sDR Body	4sDR Body L	5sDR Body R30	Group 3
	5sDR Body Care	4sDR Body Care	5sDR Body Care R30	Group 4
Scoliosis	-	4sRygg Normal dose 3D	CT Normal dose 5s R15P85	
	-	4sRygg Low dose 3D	CT Low dose 4s R15P85	

The focus-to-detector distance (FDD), when performing the CBCT, was 120 cm on *Artis Q* and *Artis Zeego* and 130 cm on *Artis Pheno*. Focus-to-reference distance (FRD), where reference is a point defined 15 cm below the center of rotation towards the x-ray tube, was 78.5 cm for all protocols on all modalities and the detector size were 40×30 cm^2. The focal spot size was large on all modalities, which represents 0.7 mm on *Artis Q* and *Artis Pheno* and 1 mm on *Artis Zeego*. On all modalities, and for all protocols the grid was used. On *Artis Q* and *Artis Zeego* the grid focus was 105 cm and on *Artis Pheno* 115 cm. The exposure and image settings for all the protocols, on each modality, are presented in Appendix A, Table A.1, A.2 and A.3. Note especially that the dose per frame (µGy/f) and 3D angle step (°/f) is changing between the protocols.

For all EVAR protocols measurements with and without collimation and zoom were made, and for the scoliosis protocols only the default (no collimation or zoom) settings were used. In Table 3.2 the different settings are presented. The collimation (C) was only available in one direction, to change the image height. For the scoliosis protocols, the image field was in portrait view, and the image width was 30 cm and the height 40 cm, on the detector. The zoom (Z) available during CBCT were 50, 42 and 32 cm for *Artis Pheno*, 48, 42 and 32 for *Artis Q* and 48 and 42 cm for *Artis Zeego.*

Table 3.2: Settings used for protocol comparison with different collimation and zoom for the modalities Artis Q, Artis Pheno and Artis Zeego. C represents the image width × image height [cm^2] on the detector after collimation and Z represents the zoom [cm].

		Modality		
	Setting	**Artis Q**	**Artis Pheno**	**Artis Zeego**
EVAR	Default	C = 40×30, Z = 48	C = 40×30, Z = 50	C = 40×30, Z = 48
	Col 1	C = 40×22, Z = 48	C = 40×24, Z = 50	C =40×22, Z = 48
	Col 2	C = 40×12, Z = 48	C = 40×12, Z = 50	C = 40×12, Z = 48
	Zoom 42	C = 26.25×26.25, Z = 42	C = 25.2×25.2, Z = 42	C =26.25×26.25, Z = 42
	Zoom 32	C = 15×15, Z = 32	C = 14.57×14.57, Z = 42	-
Scoliosis	Default	-	C = 30×40, Z = 50	C = 30×40, Z = 48

3.2.2 Image quality

The high resolution was investigated for all protocols on all modalities, listed in Table 3.1, with the default settings. Catphan was placed on the table, without the mattress, and centered at the section CTP528. The CBCT acquisition image was reconstructed with filtered back projection using the *Syngo Workplace*. The reconstruction parameters used are presented in Table 3.3. The volume of interest (VOI) size was set manually by adjusting the region of interest (ROI) so that it was covering the section that was being reconstructed (CTP528). The window level and window width was changed to receive the best setting and the number of line pairs per cm was counted.

Table 3.3: Parameters used for the reconstruction of the high-resolution module, CTP528.

Body region	Head & Neck
Job List	DCT Head Clear
VOI Size	Manual
Slice Matrix	512 × 512
Viewing Preset	VesselHead

3.3 CT

CT measurements were performed on *Discovery 750 HD,* , *General Electric Healthcare, USA*, using the abdominal phantom. The phantom was centered in the same way as for the CBCT. For EVAR there were three protocols available and for scoliosis there was one, as presented in Table 3.4. The protocol called *EVAR without contrast* (*w/o c*) + *Abdominal* (*abd.*) *aorta after EVAR* represents one scan without and one with contrast. These scans are always performed together and are therefore presented as one protocol, which contains two scans. For the first two EVAR protocols and the scoliosis protocol (*Full back*) the scan was performed over the whole abdominal phantom, from the start of the spine to the bottom of the femur bones, see Figure 3.8 (red lines). In the protocol, *Late series EVAR*, the scan was only performed over a small part of the phantom, from the iliac crest to the caput femoris, to represent a scan length performed on a real patient, see Figure 3.8 (blue box). The EVAR protocols were performed twice, first with the default settings (120 kV) and second with a changed tube voltage to 100 kV. For scoliosis the same protocol was used twice, but with a change of tube current. In the first scan, *Full back default*, using the predefined settings, meanwhile in the second, *Full back automatic*, the tube current was increased to follow the CT protocol indication, the tube voltage was 80 kV during both scans. For all of the protocols used the effective dose were calculated using CT-Expo, see section 3.7.2.

Table 3.4: Protocols for EVAR and scoliosis used for the CT scans.

	CT protocol
EVAR	Aorta before EVAR
	EVAR without contrast + abdominal aorta after EVAR
	Late series EVAR
Scoliosis	Full back

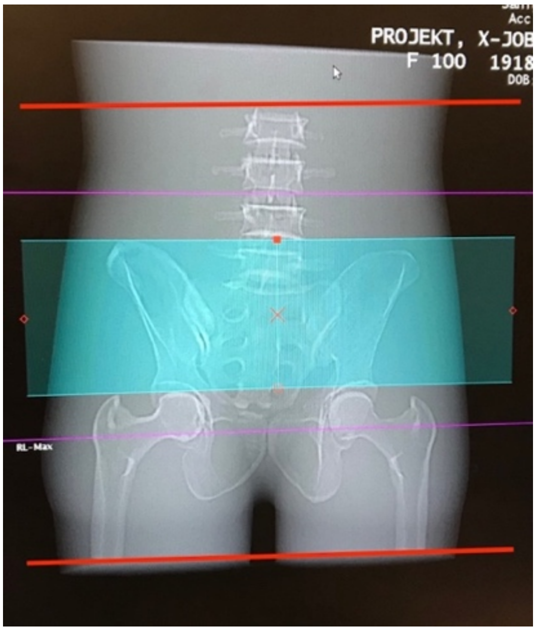

Figure 3.8: Scan lengths used for the CT protocols. The blue box represents the scan length for the late series EVAR and the red lines represents the scan range for all the other CT protocols.

3.4 Fusion

To measure the radiation dose when performing 2D fluoroscopy, for 2D-3D-fusion in EVAR procedures, the abdominal phantom was used on *Artis Q*. One low, medium and high dose fluoroscopy protocol, called *FL Low*, *FL Normal* and *FL High*, respectively, was used. The abdominal phantom was centered and one frontal and lateral exposure were performed, with no collimation or zoom and FDD = 120 cm, for all protocols. The exposure time for the fluoroscopy was set to two, four and six seconds and DAP was received. The settings used for the 2D-fluoroscopy are presented in Table 3.5.

Table 3.5: Settings used during fluoroscopy, on Artis Q, with the protocols FL Low, FL Normal and FL High.

	Fluoroscopy protocol		
Fluoroscopy setting	**FL Low**	**FL Normal**	**FL High**
X-ray tube voltage (kV)	65.5	68.4	68.0
X-ray tube current (mA)	243.4	98.6	99.4
Pulse width (ms)	12.8	10.3	12.0
Filtration (mmCu)	0.9	0.3	0.2
Pulses per second (p/s)	4	4	4

The settings for the DSA protocols are presented in Table 3.6. Each protocol consists of three phases which lasts for different times and with different frame rates.

Table 3.6: Exposure settings for the DSA protocols.

Exposure setting	**DSA Extremity 2/1/0.5**
X-ray tube voltage (kV)	70
Pulse width (ms)	200.0
Dose (µGy/f)	1.2
Min Cu filter (mmCu)	0.1
Max Cu filter (mmCu)	0.3

Phase 1	
Time (s)	6
Frame rate (f/s)	2
Phase 2	
Time (s)	40
Frame rate (f/s)	1
Phase 3	
Time (s)	18
Frame rate (f/s)	0.5

3.5 Radiation doses to personnel

To measure the radiation dose to a personnel position in a OR, the real-time personal radiation dosimetry system, *Dose Aware RaySafe i3, Unfors RaySafe AB,* Sweden, was used. By placing the dosimeters at 80, 150, 190, 270 and 310 cm from the center of the patient, see Figure 3.9, $H_p(10)$ to the personnel position during one CBCT-rotation was measured. $H_p(10)$ was measured on the modalities *Artis Q*, *Pheno* and *Zeego*, for all different protocol settings (Table 3.2).

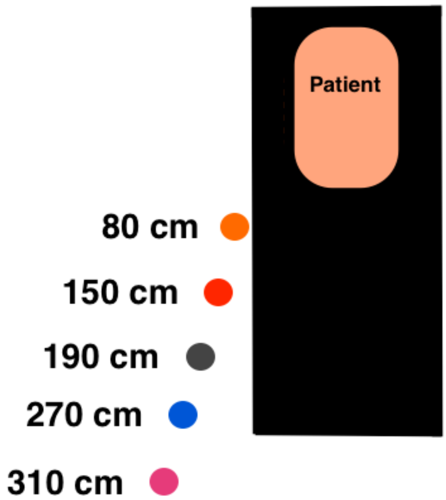

Figure 3.9: Arrangement to measure the radiation dose to a personnel position in a OR. The colored dots represent different positions for the dosimeters.

3.6 TLD-100

The TLD-100 was calibrated using the x-ray system *SUPER80CP TECH ID: SE2048, Philips Division Medicinska System, Sweden*. The radiation quality of RQA7, which is a radiation field with a tube voltage of 90 kV and a first half value layer (HVL) of 9.2 mm Aluminum [mmAl], was used [32]. During all measurements, the transmission ionization chamber, *Dose Guard 100 Dose area product meter, RTI Electronics AB, Sweden*, was used to confirm that the output of the tube was constant during all irradiations. Tube voltage and HVL was measured with the instrument *Piranha, RTI Electronics AB, Sweden,* and the soft-ware *Ocean 2014 Professional, RTI Electronics AB, Sweden*. A tube voltage as close to 90 kV as possible was set and different thicknesses of pure Al were inserted in front of the radiation field to receive an HVL of 9.2 mmAl. When the correct HVL had been determined, to represent RQA7, the air kerma was measured. The ion chamber, *Ion Chamber A3 XR122571, Exradin, USA,* and *Electrometer DIGI-X PLUS, RTI Electronics AB, Sweden*, was used to measure the air kerma, at FDD = 1 m , shown in Figure 3.10.

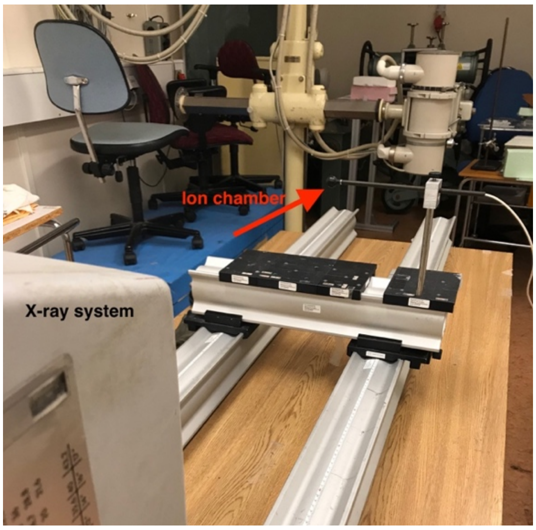

Figure 3.10: Measurement arrangement of the kerma measurements free in air.
The arrow shows the ion chamber and the x-ray system is shown in the bottom left corner in the figure.

The measured charge from the ion chamber was corrected for temperature and pressure and multiplied with the interpolated calibration factor, from the calibration certificate, to receive the absorbed dose in air [mGy]. After the measurements of air kerma with the ion chamber, TLDs were irradiated. The TLDs were placed in five holes, see Figure 3.11, in the center of a slice of PMMA ($0.2 \times 25 \times 30$ cm^3), positioned in the center of the radiation field. The TLD-100 were irradiated at the same position as the ion chamber, at FDD = 1 m, with no material behind the PMMA slice, representing a free in air measurement, and at the surface of a 15 cm thick PMMA phantom. After irradiation, the TLDs were read out with *HARSHAW TLD 6600 PLUS Thermo Scientific, USA,* and the software *WinHPRS*.

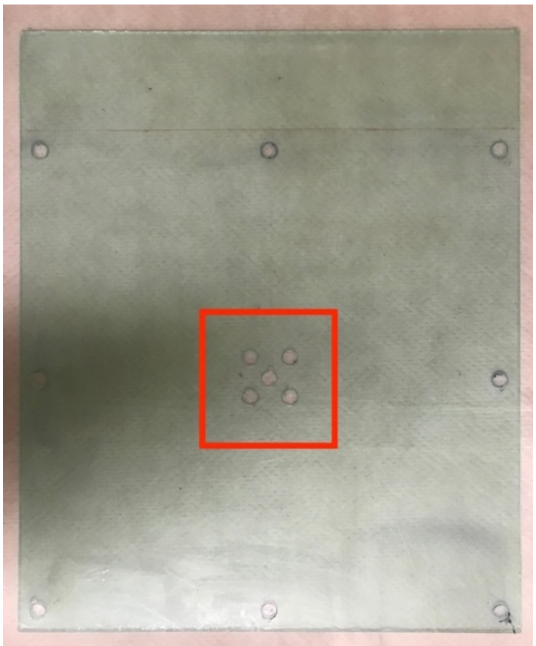

Figure 3.11: Positions of the dosimeters, TLD-100, at the calibration.

To estimate the absorbed dose of the TLDs at the surface of the 15 cm thick PMMA phantom Eq. (9) was used [33].

$$D_{PMMA} = D_{air} \cdot BSF \cdot \left(\frac{\mu_{en}}{\rho}\right)_{air}^{PMMA,60.7\ keV} \quad (9)$$

Where, D_{PMMA}, is the estimated absorbed dose in PMMA, D_{air} is the absorbed dose in air at FDD = 1m, BSF is the backscatter factor and, $\left(\frac{\mu_{en}}{\rho}\right)_{air}^{PMMA,60.7\ keV}$, is the quotient of the tabulated mass energy-absorption coefficients between PMMA and water at the photon energy of 60.7 keV and is 0.84. The BSF was determined by the quotient of the TLD charge at the surface of the 15 cm thick PMMA phantom and the charge measured free in air at FDD = 1 m. The mean photon energy, 60.7 keV, was determined using *Siemens Healthineers Simulation of X-ray Spectra* [34]. By inserting the tube voltage (90 kV) and used filtration (9.2 mmAl) the x-ray spectrum was calculated, and the mean photon energy decided. The calibration factor [nC/µGy] for the TLDs was determined by the quotient between the measured charge of the TLDs and the estimated absorbed dose (D_{PMMA}), to the TLDs.

When using TLD-100, to measure the radiation dose, the PMMA and abdominal phantom were used. The TLDs were placed in the PMMA phantom and on the surface of the abdominal phantom, as described in section 3.1. The TLD measurements were made on *Artis Q* with the protocols for EVAR, see Table 3.1. To be able to perform the CBCT, first, a short time of fluoroscopy was needed so that the modality could adjust the exposure parameters before the rotation. At this fluoroscopy 0.5 pulses/second was used and the fluoroscopy time was held as short as possible. Thereafter, the CBCT was performed. After the rotation, all the TLDs were exchanged and a new measurement, with a different protocol, was performed. The steps were repeated until all the protocols had been measured. The same steps were then repeated with the abdominal phantom. The dosimeters were read out with *HARSHAW TLD 6600 PLUS Thermo Scientific, USA,* and the software *WinHPRS*, using the calibration factor that earlier had been determined. The signal was corrected for background radiation.

3.7 Effective dose

3.7.1 PCXMC20Rotation

PCXMC20Rotation was used to calculate effective doses from the CBCT on the abdominal phantom. In this study, calculations were made with the weighting factors from ICRP 103. The examination data for the CBCT exposures were collected from the DICOM data, using *DicomEdit 7.0 Siemens*. By inserting the data in a PCXMC excel spreadsheet the effective doses were calculated using a macro. The patient's height, weight and age was set to be 175 cm, 73 kg and 30 years, respectively. Table 3.7 shows an example of the data needed to perform a macro.

Table 3.7: Example of input data in PCXMC20Rotation to calculate effective dose. Each row represents one projection angle.

Hospital	Examination	Projection (num.angle)	Oblique angle	Patient number
A	Abdomen	352.5	0	1
A	Abdomen	354.1	0	1
A	Abdomen	355.6	0	1

Patient height (cm)	Patient weight (kg)	Patient age	X-ray tube voltage (kV)	Filtration (mmAl)
175	73	30	90	3.1
175	73	30	90	3.1
175	73	30	90	3.1

Additional filtration (mmCu)	Focus-to-reference distance (FRD)	X-ray beam width at FRD (cm)	X-ray beam height at FRD (cm)	X-ref
0	78.5	26.21	19.66	0
0	78.5	26.21	19.66	0
0	78.5	26.21	19.66	0

Y-ref	Z-ref	Arms in phantom (1 or 0)	Input dose quantity	Input dose value
0	20	0	MAS	3.759
0	20	0	MAS	3.759
0	20	0	MAS	3.119

Each row of data represents one projection angle. The projection angle was recalculated from DICOM-standard to PCXMC standard because the angle is presented in different ways, see Table 3.8. The filtration [mmAl] represents the total filtration of the used modality. The x-ray tube voltage [kV] and additional filtration mm Copper [mmCu] were received from the DICOM data The X-ray beam width and height were calculated using PCXMC20Rotation by inserting FRD, FDD and detector size that was used for the CBCT. *X-ref*, *Y-ref* and *Z-ref* represent the coordinates were the field enter the patient and was set to (0:0:20). Figure 3.12 shows the position in the PCXMC-phantom. To calculate the total effective dose a summation of the effective dose for each projection angle was made. For some protocols and settings measurements were made more than once, and a mean value was then calculated.

Table 3.8: Presentation of angle for PCXMC and DICOM.

PCXMC angle	DICOM angle
0	-90
270	-180
180	90
90	0

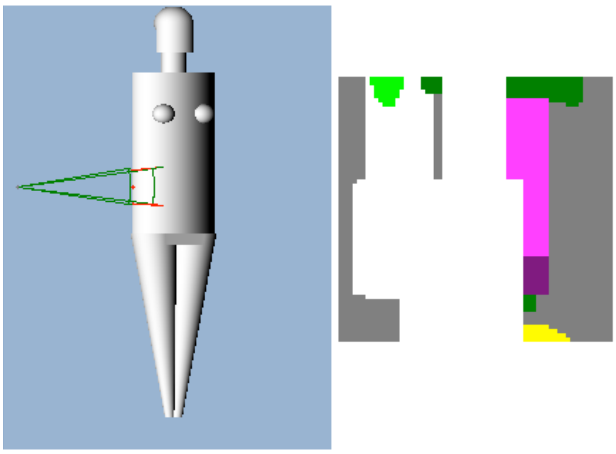

Figure 3.12: The left figure represents one of the radiation field positions in the mathematical phantom in PCXMC20Rotation and the right shows the irradiated organs. Both figures are screenshots from PCXMC20Rotation.

3.7.2 CT-Expo

To calculate the effective doses from the CT scans, CT-Expo v2.5 was used. In the calculations, the weighting factors from ICRP 103 was used. The CT manufacturer and scanner was selected and scan parameters, such as scan range and tube voltage [kV] was inserted in the calculation sheet, se Table 3.9. The DICOM data were retrieved using *Micro Dicom viewer* and to collect values from specific DICOM tags a homemade program, *Tagga Ner*, was used. The scan parameters were collected from the DICOM data and the tube current [mA] used for calculation was the mean tube current indicated. Table 3.9 shows an example of scan parameters used for calculation, where

Table 3.9: Example of scan parameters inserted in CT-Expo.

U [kV]	I [mA]	t [s]	Q_{el} [mAs]	$N \cdot h_{col}$ [mm]	TF [mm]	H_{rec} [mm]	p	Ser.
120	167	0.4	67	40.0	39.4	0.6	0.98	1

U represents the tube voltage, *I* the electrical tube current, *t* the acquisition time per slice, Q_{el} is the product of *I* and *t*, $N \cdot h_{col}$ is the beam width, *TF* is the table feed per rotation, H_{rec} is the reconstructed slice thickness and *p* is the pitch factor and *Ser.* is the number of scan series. The phantom used in the calculation represents an adult man with a length of 170 cm and the weight of 70 kg. Calculations were performed for all the CT scans with the scan lengths used during CT imaging, and also with the scan lengths used during the previously performed CBCT. The scan lengths are presented in Table 3.10.

Table 3.10: Scan range used for calculations of effective dose with CT-Expo for each of the protocols.

	CT protocol	CT scan range [cm]	CBCT scan range [cm]
EVAR	Aorta before EVAR	33	19
	EVAR without contrast + abdominal aorta after EVAR	33	19
	Late series EVAR	11	19
Scoliosis	Full back	33	25

The centering of the radiation field was manually set in CT-Expo to represent the real scan range. In Figure 3.13 the positioning of the CT scan range and the CBCT scan range are shown, respectively. In Figure 3.13a the left image represents 33 cm scan range and the right image 11 cm. In Figure 3.13b the left image represents 19 cm and the right 25 cm.

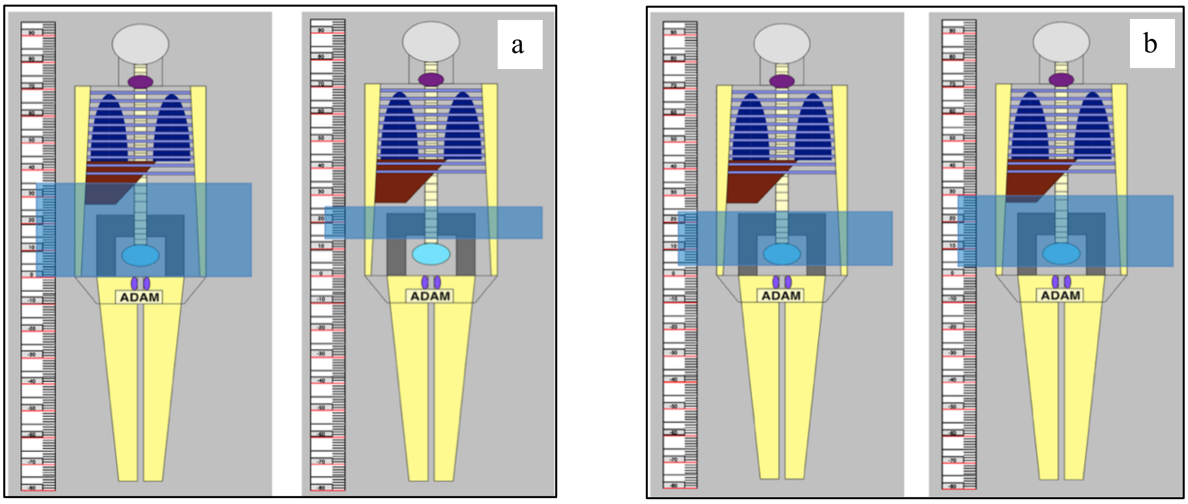

Figure 3.13: The positioning of the radiation field for a: the 33 cm (left) and 11 cm (right) CT scan range and, b: the 19 cm (left) and 25 cm (right) CBCT scan range.

3.8 Statistical analysis

The statistical analysis was performed with one-tailed distribution *T.TEST* (*Microsoft Excel*), for the calculations of protocol difference, with a significance level, α = 0.05. For the calculations of significance between different modalities, a two-tailed test was used, with the significance level, α = 0.05.

4 Results

4.1 EVAR

4.1.1 Protocol Comparison

4.1.1.1 Radiation dose

In Appendix B, Table B.1, B.2 and B.3, the radiation doses using the EVAR CBCT protocols are presented for all settings and protocols on the different modalities, received from one CBCT using the abdominal phantom. The radiation doses presented are DAP [$Gycm^2$], DAP per detector area, DAP/A [mGy], IAK in the reference point, $D_{skin,DICOM}$ [mGy], and absorbed dose rate, $\dot{D}$ [mGy/s], effective dose, E [mSv], and absorbed doses, $D_{skin,PCXMC}$, $D_{active\ bone\ marrow}$ (D_{ABM}), D_{colon}, $D_{kidneys}$, $D_{ovaries}$ and $D_{small\ intestine}$ (D_{SI}) [mGy]. The effective dose [mSv] on the modalities *Artis Q*, *Pheno* and *Zeego*, for all settings, are presented in Figure 4.1a-c. An increased collimation resulted in a decreased effective dose. Also, with an increased zoom the effective dose decreased. The effective dose using the default (no collimation or zoom, see Table 3.2) setting was on average a factor 1.1±0.017, 1.8±0.14, 1.3±0.054 and 2.0±0.26 higher than the effective dose using, collimation 1, collimation 2, zoom 42 and zoom 32, respectively.

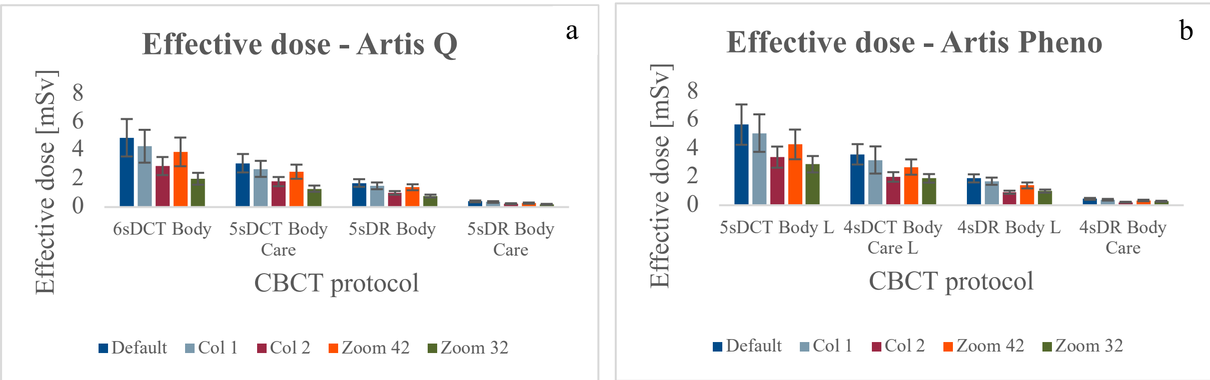

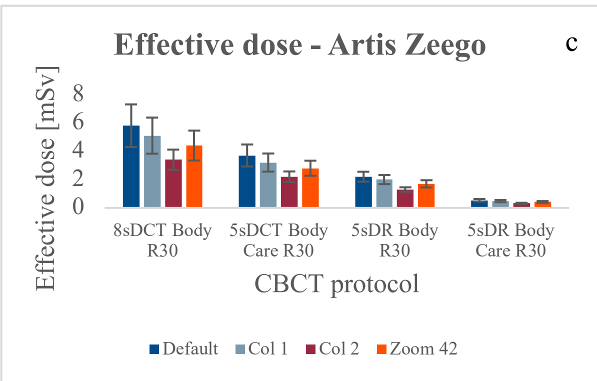

Figure 4.1: Effective dose[mSv] for all CBCT protocols and settings on Artis Q, Artis Pheno and Artis Zeego, using the abdominal phantom. Figure a: 6sDCT Body, 5sDCT Body Care, 5sDR Body and 5sDR Body Care on Artis Q, b: 5sDCT Body L, 4sDCT Body Care L, 4sDR Body L and 4sDR Body Care on Artis Pheno and c: 8sDCT Body R30, 5sDCT Body Care R30, 5sDR Body R30 and 5sDR Body Care R30 on Artis Zeego. The error bars indicate the uncertainties with PCXMC20Rotation.

The effective dose using the default settings, for the same protocols on different modalities, are presented in Figure 4.2. Protocol group 1, 2, 3 and 4, respectively, were to be representative in radiation dose on the different modalities, where group 1 were: *6sDCT Body*, *5sDCT Body L* and *8sDCT Body R30*, group 2: *5sDCTBody Care*, *4sDCT Body Care L* and *5sDCT Body R30*, group 3: *5sDR Body*, *4sDR Body L* and *5sDR Body R30* and group 4: *5sDR Body Care*, *4sDR Body Care* and *5sDR Body Care R30*, on *Artis Q*, *Pheno* and *Zeego*, respectively, see Table 3.1. In Appendix B, Figure B.1a-d, the effective dose using the CBCT EVAR protocols with the settings collimation 1 and 2 and zoom 42 and 32 are presented. The lowest effective dose was received using *Artis Q*, for all protocols and settings.

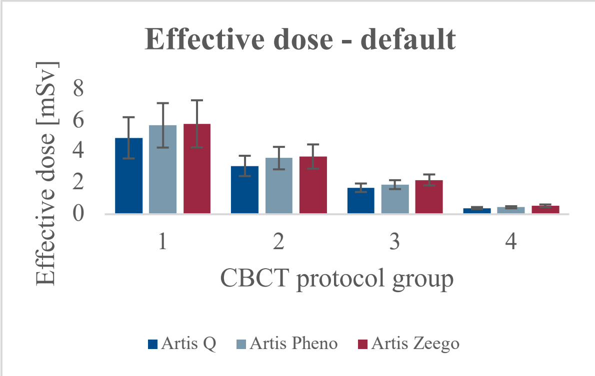

Figure 4.2: Effective dose [mSv] for the CBCT EVAR protocols, using the default setting and the abdominal phantom for all protocols on Artis Q, Artis Pheno and Artis Zeego. Group 1: 6sDCT Body, 5sDCT Body L and 8sDCT Body R30, group 2: 5sDCTBody Care, 4sDCT Body Care L and 5sDCT Body Care R30, group 3: 5sDR Body, 4sDR Body L and 5sDR Body R30 and group 4: 5sDR Body Care, 4sDR Body Care and 5sDR Body Care R30, on Artis Q, Artis Pheno and Artis Zeego, respectively. The error bars indicate the uncertainties with PCXMC20Rotation.

In Appendix B, Table B.4, B.5 and B.6, the relative difference of DAP [Gycm^2], DAP/A [mGy], $D_{skin,DICOM}$ [mGy], $\dot{D}$ [mGy/s], E [mSv], $D_{skin,PCXMC}$, D_{ABM}, D_{colon}, $D_{kidneys}$, $D_{ovaries}$ and D_{SI} [mGy], between the protocols, compared to the low dose protocol on each modality, group 4, are shown, respectively. The maximum relative difference in effective dose, for all modalities and settings, was a factor 16, 9.0 and 4.8, for the high dose protocols (group 1), second highest dose protocols (group 2) and for the second lowest dose protocols (group 3), respectively. All EVAR CBCT protocols on *Artis Q* and *Artis Pheno* were significantly different (p-value<0.05), when comparing the default settings, and the values for DAP, $D_{skin,DICOM}$, $\dot{D}$, E, $D_{skin,PCXMC}$, D_{ABM}, D_{colon}, $D_{kidneys}$, $D_{ovaries}$ and D_{SI}.

In Appendix B, Table B.7-B.10, the percentage difference in radiation dose for the same protocols and settings (collimation and zoom) on the different modalities, *Artis Q*, *Pheno* and *Zeego*, are presented. The corresponding protocols on *Artis Pheno* and *Artis Zeeg*o has been compared to *Artis Q*. Note that some values are small and close to each other, see Appendix B, Table B.1-B.3, which results in a large percentage difference.

4.1.1.2 Image quality

The number of line pairs per cm did not vary between different EVAR protocols and modalities. For all protocols, 8 or 9 lp/cm was seen, with no correlation between different protocols. Figure 4.3 shows the line pair per cm for two protocols. The left figure shows 8 lp/cm and the right 9 lp/cm.

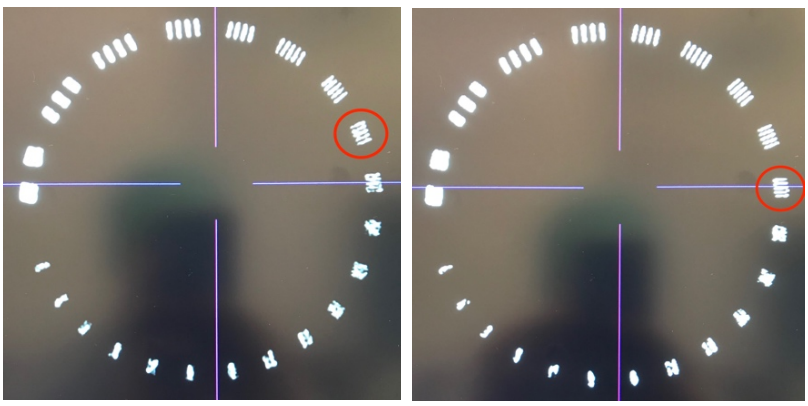

Figure 4.3: Schematic image of the number of line pairs per cm after a CBCT on Artis Q, Pheno and Zeego. The left figure represents 8 lp/cm and the right 9 lp/cm.

4.1.2 CT

In Figure 4.4 the calculated effective dose [mSv] for the protocols used for CT with different settings is presented. For the protocols *Aorta before EVAR*, *EVAR without contrast* and *abdominal aorta after EVAR* the radiation dose increased with decreased tube voltage. When the smaller scan range for the CBCT was used for these protocols the radiation dose decreased, as expected. While for *Late series EVAR* the radiation dose instead decreased when using the lower tube voltage, but as expected increased with the, here increased, scan range of the CBCT. One scan with the protocol *Aorta before EVAR* gave the same radiation dose as one scan with *EVAR without contrast* or *Abdominal aorta after EVAR*, if the same scan range was used. Therefore, the effective dose was doubled when the two protocols, *EVAR without contrast + Abdominal aorta after EVAR,* were used, in combination. With *Late series EVAR* a lower effective dose was received, compared to the other protocols. In Appendix B, Table B.11, the radiation dose quantities, $CTDI_{vol}$, DLP, effective dose and equivalent organ doses are presented, for all CT EVAR protocols and settings.

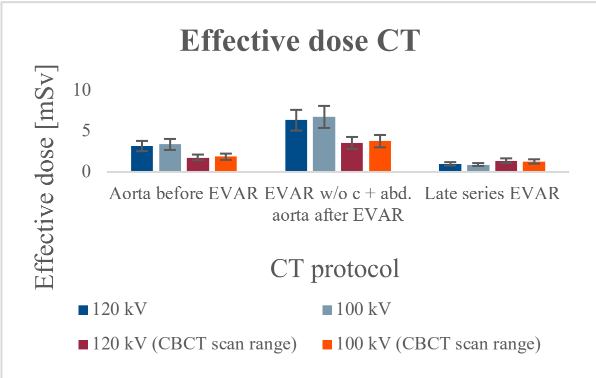

Figure 4.4: Effective dose [mSv] for CT EVAR protocols, with different settings, using the abdominal phantom. The error bars indicate the uncertainties with CT-Expo.

4.1.3 CBCT vs CT

The relative difference between the effective doses using the CBCT EVAR protocols with the default setting and the CT EVAR protocols with different settings, are presented in Table 4.1. For the two high radiation dose CBCT protocols, on all modalities, group 1 and 2, respectively, the effective dose from the CBCT was a factor 1.1-3.2 higher, compared to the CT protocol *Aorta before EVAR*, using both CT settings. However, when *5sDCT Body Care* on *Artis Q* was compared with the effective dose from the CT protocol *Aorta before EVAR 120 kV* and *100 kV*, it gave a factor 1.0 and 0.9, respectively. The effective dose for the two low radiation dose CBCT protocols, on all modalities, group 3 and 4, compared to *Aorta before EVAR 120 kV* and *100 kV* using the CBCT scan range, was a factor 0.12-0.93 lower for the CBCT protocols, except for the protocols *4sDR Body L* and *5sDR Body R3*0 (group 3), which gave a factor 1 and 1.2. For all of the CBCT protocols compared to the CT protocols *EVAR without contrast + abdominal aorta after EVAR*, except for the highest radiation dose protocols, group 1, using the CBCT scan range, the quotient was smaller than or equal to one (a factor 0.059-1). For the *Late series EVAR* the opposite is shown, the effective dose from the CBCT was a factor 1.2-6.5 higher, for all CBCT protocols on all modalities, except for the low dose CBCT protocols, group 4*,* on *Artis Q, Pheno* and *Zeego,* respectively, which were a factor 0.29-0.6 lower.

*Table 4.1: Relative effective doses between the CBCT EVAR protocols, with default settings, and CT EVAR protocols with different settings, using the abdominal phantom. * CBCT scan range has been used.*

		CBCT modality and EVAR protocol											
		Artis Q	**Artis Pheno**	**Artis Zeego**	**Artis Q**	**Artis Pheno**	**Artis Zeego**	**Artis Q**	**Artis Pheno**	**Artis Zeego**	**Artis Q**	**Artis Pheno**	**Artis Zeego**
		Group 1			**Group 2**			**Group 3**			**Group 4**		
CT EVAR protocol	**Setting**	**6sDCT Body**	**5sDCT Body L**	**8sDCT Body R30**	**5sDCT Body Care**	**4sDCT Body Care L**	**5sDCT Body Care R30**	**5sDR Body**	**4sDR Body L**	**5sDR Body R30**	**5sDR Body Care**	**4sDR Body Care**	**5sDR Body Care R30**
Aorta before EVAR	120 kV	1.5	1.8	1.8	1.0	1.1	1.2	0.52	0.59	0.70	0.13	0.14	0.17
	100 kV	1.4	1.7	1.7	0.90	1.1	1.1	0.49	0.55	0.65	0.12	0.13	0.16
	*120 kV	2.7	3.2	3.2	1.7	2.0	2.1	0.93	1.0	1.2	0.22	0.25	0.30
	*100 kV	2.6	3.0	3.1	1.6	1.9	2.0	0.88	1.0	1.2	0.21	0.24	0.29
EVAR w/o c + abd. aorta after EVAR	120 kV	0.76	0.89	0.91	0.48	0.56	0.58	0.26	0.29	0.35	0.063	0.070	0.085
	100 kV	0.72	0.84	0.86	0.45	0.53	0.55	0.25	0.28	0.33	0.059	0.066	0.080
	*120 kV	1.4	1.6	1.6	0.85	0.99	1.0	0.47	0.52	0.62	0.11	0.12	0.15
	*100 kV	1.3	1.5	1.5	0.80	0.94	0.98	0.44	0.50	0.59	0.11	0.12	0.14
Late series EVAR	120 kV	4.9	5.7	5.8	3.1	3.6	3.7	1.7	1.9	2.2	0.40	0.45	0.54
	100 kV	5.4	6.3	6.5	3.4	4.0	4.2	1.9	2.1	2.5	0.45	0.50	0.60
	*120 kV	3.5	4.1	4.2	2.2	2.6	2.7	1.2	1.3	1.6	0.29	0.32	0.39
	*100 kV	3.7	4.4	4.5	2.4	2.8	2.9	1.3	1.4	1.7	0.31	0.34	0.42

4.1.4 Fusion

In Table 4.2 DAP received from fluoroscopy, with different fluoroscopy times, is shown. Using a longer fluoroscopy time, the DAP increased linearly. In the lateral direction, the received DAP is higher compared to the frontal direction. DAP increased with the fluoroscopy protocols FL Low, FL Normal and FL High, as expected.

Table 4.2: DAP [Gycm^2] for different times of fluoroscopy with the protocols FL Low, FL Normal and FL high on Artis Q, using the abdominal phantom.

		DAP [Gycm^2]		
		Fluoroscopy time		
Protocol	**Position**	**2 s**	**4 s**	**6 s**
FL Low	Frontal	0.027	0.052	0.079
	Lateral	0.084	0.16	0.26
	Summation	0.11	0.21	0.34
FL Normal	Frontal	0.056	0.12	0.16
	Lateral	0.13	0.26	0.38
	Summation	0.18	0.38	0.54
FL High	Frontal	0.10	0.19	0.27
	Lateral	0.22	0.44	0.64
	Summation	0.31	0.63	0.91

The total DAP received from all the different phases of the protocol *DSA Extremity 2/1/0.5* is 41 Gycm^2. In Table 4.3 the contribution, to DAP, from each phase is presented. From phase 2 the highest DAP was received. Also, a factor 2.2 higher DAP was received when the lateral direction was used.

Table 4.3: DAP [Gycm^2] received from each phase with the protocol DSA Extremity 2/1/0.5, on Artis Q, using the abdominal phantom.

		DAP [Gycm^2]		
Protocol	**Position**	**Phase 1**	**Phase 2**	**Phase 3**
DSA Extremity 2/1/0.5	Frontal	2.5	8.3	1.9
	Lateral	5.6	19	4.2
	Summation	8.1	27	6.0

When comparing DAP received from fluoroscopy and DSA with the radiation dose received during CBCT, a factor 10 lower DAP is received, when comparing six seconds fluoroscopy, with the protocol *FL Low* (Table 4.2), and a factor 12 higher DAP is received, when comparing the sum of all phases *DSA Extremity 2/1/0.5*, with the low radiation dose CBCT protocol, *5sDR Body Care* (group 4), on *Artis Q* (Appendix B, Table B.1).

4.1.5 Tube output

When evaluating the effective dose, it was found that for *Artis Q,* using default settings gave the lowest tube current-exposure time product [mAs] for all projections. In Figure 4.5a the tube current-exposure time product for *5sDR Body Care* (group 4, *Artis Q*) is presented. A similar curve was received for the protocol *5sDR Body* (group 3), as seen in Figure 4.5b, even if an increase in tube current-exposure time product was seen, leading to an increase in effective dose, if the other parameters are unchanged. The tube current-exposure time product for the protocol *6sDCT Body* (group 1) is shown in Figure 4.5c, for different projections, a similar curve was received for the protocol *5sDCT Body Care* (group 2). If instead looking at the tube voltage [kV], generally the tube voltage was 90 kV for all projections, using all protocols. Interestingly, for *6sDCT Body* and *5sDCT Body Care* (group 1 and 2) an increase in tube voltage, to a maximum of 108 kV, was seen for the projections outside the middle section (the posterior-anterior direction, -30° to 30°), but only for the settings collimation 2, zoom 42 and zoom 32, as shown in Figure 4.5d. For those protocols a correlation between the tube current-exposure time product and tube voltage was seen. An increase in tube current-exposure time product resulted in a decrease in tube voltage, and a decrease in tube current-exposure time product in an increased tube voltage.

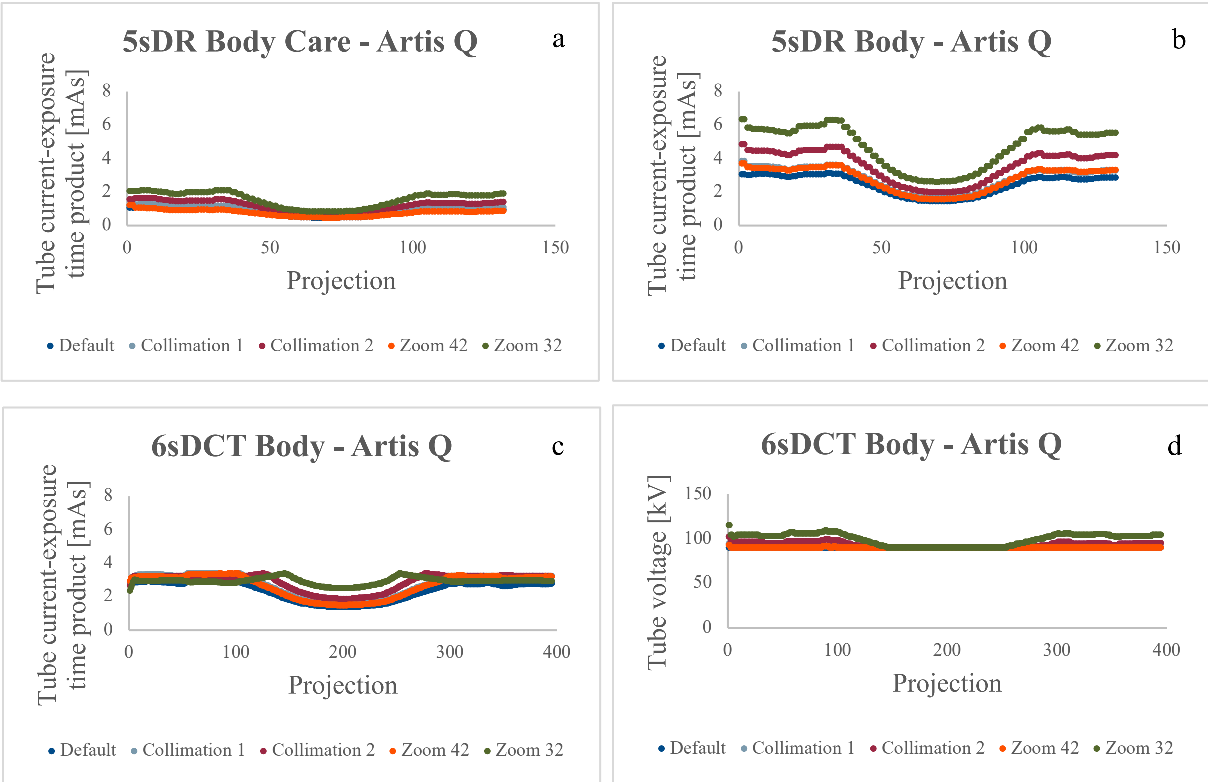

Figure 4.5: Tube current-exposure time product [mAs] at different projections, for all settings and protocols on Artis Q, using the abdominal phantom. In figure a, b and c the tube current-exposure time product [mAs] for 5sDR Body Care, 5sDR Body and 6sDCT Body is presented, respectively. The protocol 5sDCT Body Care is also represented by figure c. Figure d presents the change in tube voltage [kV] at different projections with the protocol 6sDCT Body. Note that the number of projections differ between the protocols.

In Figure 4.6a the tube current-exposure time product for the protocol *4sDR Body Care* (group 4, Artis Pheno) is presented. As for the same protocol on *Artis Q*, zoom 32 gave the highest tube current-exposure time product. Figure 4.6b and c show the tube current-exposure time product and tube voltage, at different projections for the protocol *5sDCT Body L* (group 1), which also was representative for the protocols *4sDR Body L* and *4sDCT Body Care L* (group 3 and 2, respectively). With zoom 32 a reverse tube current-exposure time product was seen compared to the other settings. Outside the posterior-anterior direction, the tube current-exposure time product for zoom 32 was higher than for all of the other settings, and in the posterior-anterior direction, it was decreased below the tube current-exposure time product for zoom 42 and collimation 2. In the posterior-anterior direction, a decrease in tube current-exposure time product was seen for all protocols and settings on *Artis Pheno*, but it was still higher than outside this area. This differed compared to the protocols on *Artis Q*, where the tube current-exposure time product was at its lowest in the posterior-anterior direction. For all settings on all protocols, except for zoom 32 on *5sDCT Body L, 4sDR Body L* and *4sDCT Body Care*, the tube voltage was 90 kV. For zoom 32 the tube voltage was increased in the posterior-anterior direction. As for the protocols on *Artis Q*, using zoom 32, a correlation between tube current-exposure time product and tube voltage was seen.

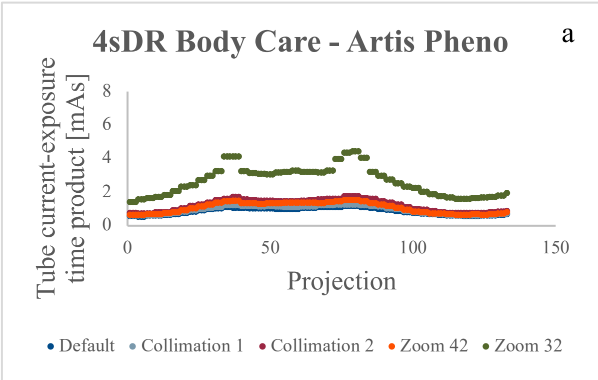

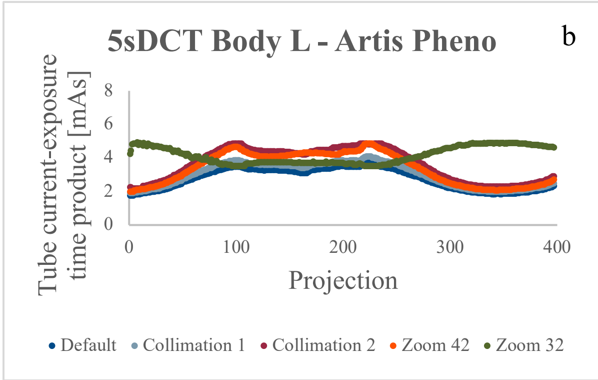

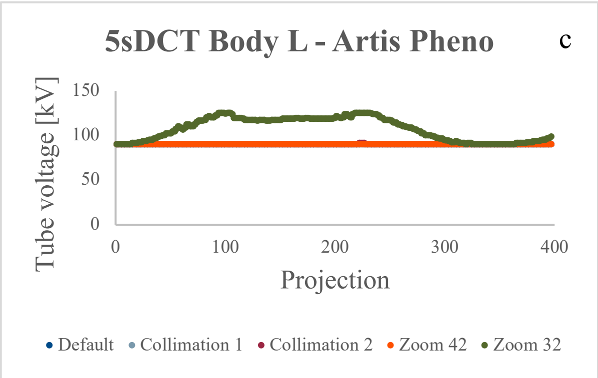

Figure 4.6: Tube current-exposure time product [mAs] at different projections, for all settings and protocols on Artis Pheno, using the abdominal phantom. In figure a and b the tube current-exposure time product [mAs] for the protocols 4sDR Body Care and 5sDCT Body L is presented, respectively. Tube voltage [kV] at different projections, for the protocol 5sDCT Body L, is seen in figure c. The protocols 4sDR Body L and 4sDCT Body Care L is represented by figure b and c. Note that the number of projections differ between the protocols.

The tube current-exposure time product for the protocols, *5sDR Body Care R30* and *5sDR Body R30* (group 4 and 3, respectively, on *Artis Zeego*), is presented in Figure 4.7a and b. A decrease in tube current-exposure time product was seen in the posterior-anterior direction for both protocols, but for *5sDR Body R30* the current was increased in amplitude. With the default setting the lowest tube current-exposure time product was received. The curves for tube current-exposure time product and tube voltage, for the protocols *5sDCT Body Care R30* and *8sDCT Body R30* (group 2 and 1, respectively), is represented by Figure 4.7c and d. By using collimation 2 the highest tube current-exposure time product was received in all projections for group 3 and 4 and in the posterior-anterior direction for group 1 and 2. At the other projection the tube current-exposure time for collimation 2 was decreased and gave the lowest tube current. The tube voltage for group 4 and 3 was 90 kV for all settings and projections. However, for group 1 and 2, the tube voltage was changing. The tube voltage was decreased in the posterior-anterior direction and a correlation with tube current-exposure time product and tube voltage was also seen for these protocols, as previously mentioned.

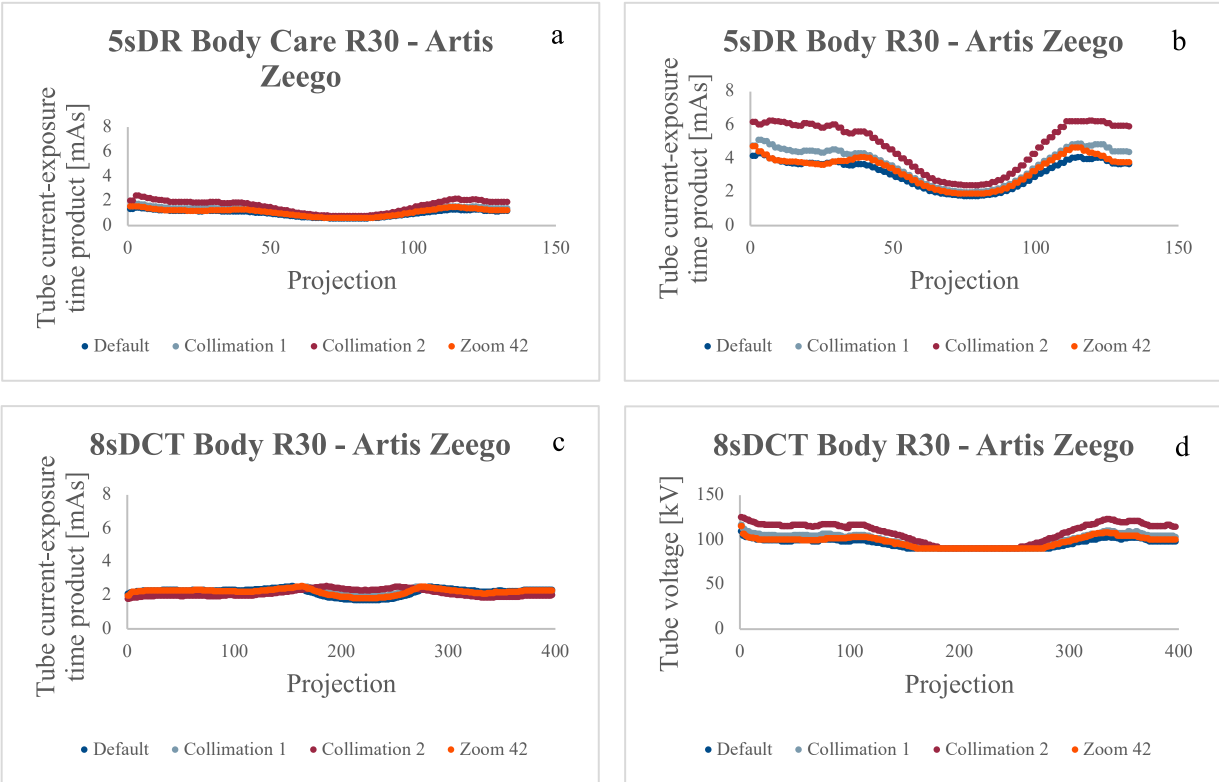

Figure 4.7: Tube current-exposure time product [mAs] at different projections, for all settings and protocols on Artis Zeego, using the abdominal phantom. In figure a, b and c the tube current-exposure time product [mAs] for the protocols5sDR Body Care R30, 5sDR Body R30 and 8sDCT Body R30 is presented, respectively. In figure d the tube voltage [kV] at different projections is presented, for the protocol 8sDCT Body R30. Figure c and d also represents the protocol 5sDCT Body Care R30.

4.1.6 Radiation dose to personnel

In Figure 4.8a-c the radiation dose to a personnel dosimeter position during one CBCT with default settings for *Artis Q, Pheno* and *Zeego*, is shown. The radiation dose is presented at different distances from the center of the patient, for the EVAR protocols. The further away from the patient the personnel stands the smaller radiation dose was received. The highest radiation dose was given by the protocols in group 1 and the lowest by group 4, on *Artis Q, Pheno* and *Zeego*, respectively.

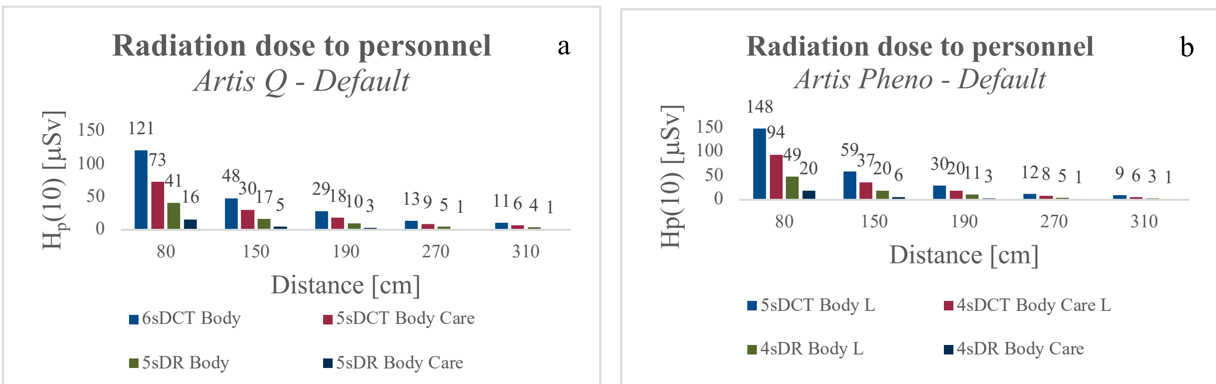

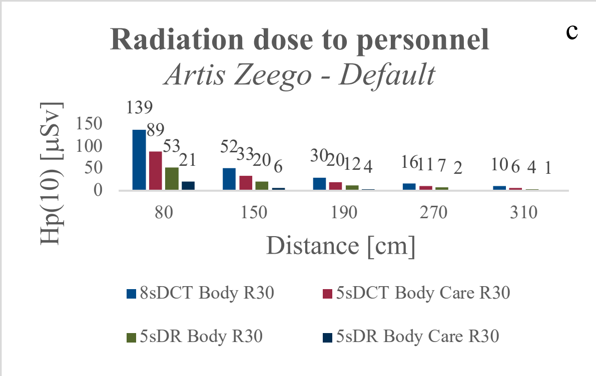

Figure 4.8: Estimated radiation dose, $H_p(10)$ [µSv], to personnel during one CBCT, with the default settings and the CBCT protocols EVAR, at different distances from the center of the patient, on a: Artis Q, b: Artis Pheno and c: Artis Zeego.

When collimation or zoom was used compared to the default settings, the estimated radiation dose to the personnel dosimeter position was decreased compared to the default settings, as seen in Appendix C, Table C.1-C.4, C.5-8 and C.9-11, on the modalities *Artis Q*, *Pheno* and *Zeego*, respectively. The values at the distance 190 cm, for all protocols on Artis Pheno, is not presented because the dosimeter had fallen on the floor during the measurements. It was shown that, for all CBCT protocols on all modalities, except for the second lowest radiation dose protocol *5sDR Body R30* (group 3) on *Artis Zeego* at the distance 80 cm using collimation 1, the estimated personnel radiation dose was decreased with more collimation. If instead looking at the percentage difference in radiation dose to a personnel position, when zoom is used, it was seen that the radiation dose decreases for all protocols on all modalities with increased zoom, except when using zoom 42 on *Artis Pheno* with the high radiation dose protocol *5sDCT Body L* (group 1) at the distance 80 cm. In contrast to the above, when using zoom 32 on *Artis Q* with the second lowest radiation dose protocol *5sDR Body* (group 3) at the distances 80 and 190 cm, and for all protocols on *Artis Pheno* at the distance 80 cm and for the low radiation dose protocol *4sDR Body Care* (group 4) at the distance 150 cm, the radiation dose to a personnel dosimeter position instead increased.

4.1.7 TLD-100

The absorbed dose in air, D_{air}, was determined to 0.63 mGy and BSF to 1.8. The absorbed dose in PMMA, D_{PMMA}, was determined to 0.97 mGy and the mean calibration factor set to 0.036 nC/µGy. The absorbed dose [mGy] from the TLD-100 measurements, with the PMMA phantom and the abdominal phantom, during one CBCT with the EVAR protocols on Artis Q, are presented in Table 4.4 and Table 4.5. It was shown that the highest absorbed dose is received with the protocol *6sDCT Body* (group 1) and the lowest with *5sDR Body Care* (group 4), using the PMMA phantom and the abdominal phantom, respectively. The mean relative difference, between the high and low dose protocol, for all of the positions in the PMMA phantom and the abdominal phantom, was a factor 12±1.9 and 14±1.0. The second highest absorbed dose was received from *5sDCT Body Care* (group 2) and the second lowest from *5sDR Body* (group 3). Comparing *5sDCT Body Care* to *5sDR Body Care*, the absorbed dose was a factor 7.5±1.2 or 8.3±0.94 higher, when measured with the PMMA phantom or the abdominal phantom. For the protocol *5sDR Body* (group 3) the absorbed dose was 4.1±0.6 times higher with the PMMA phantom and 4.8±0.36 times higher with the abdominal phantom, compared to *5sDR Body Care* (group 4). The TLD-position that receives the highest absorbed dose, measured with the PMMA phantom, for all the protocols was the left side TL-dosimeter. If instead the absorbed dose to the TLD-position in different PMMA-planes are compared, the TLD-positions 4, 5 and 6 (mid positions in the right-left direction) on each plane received the highest absorbed dose, marked with a red box in Table 4.4.

Table 4.4: Absorbed dose [mGy] from TLD-100 measurements with the PMMA phantom. The absorbed doses are received for one CBCT-rotation with the EVAR protocols on Artis Q. The cells within the red box have received a higher absorbed dose than the rest of the TLD in that plane.

	Absorbed dose [mGy] of TLD on Artis Q			
	CBCT protocol			
TLD position	**6sDCT Body**	**5sDCT Body Care**	**5sDR Body**	**5sDR Body Care**
1.1	1.1	0.80	0.44	0.11
1.2	1.4	0.90	0.48	0.17
1.3	1.8	1.1	0.63	0.16
1.4	7.4	5.2	2.5	0.61
1.5	4.6	2.8	1.6	0.42
1.6	15	9.1	5.0	1.1
1.7	1.2	0.64	0.36	0.13
1.8	1.2	0.65	0.37	0.12
1.9	1.3	0.75	0.46	0.11
2.1	1.5	1.3	0.61	0.25
2.2	2.0	1.5	0.73	0.21
2.3	2.3	1.6	0.90	0.20
2.4	12	7.8	4.7	1.1
2.5	6.0	3.8	2.3	0.53
2.6	21	14	7.5	1.7
2.7	1.6	0.84	0.60	0.12
2.8	1.9	1.0	0.59	0.15
2.9	1.7	1.0	0.57	0,17
3,1	3.1	2,5	1,1	0.29
3.2	3.7	2.7	1.4	0.38
3.3	4.5	3.2	1.7	0.40
3.4	31	20	11	2.6
3.5	13	8.1	4.5	1.1
3.6	45	29	15	3.4
3.7	3.1	1.6	1.0	0.22
3.8	3.6	2.0	1.1	0.31
3.9	3.0	1.8	1.0	0.27
4.1	3.9	2.9	1.6	0.39
4.2	5.5	3.6	1.9	0.48
4.3	5.2	3.9	2.0	0.48
4.4	39	24	15	2.8
4.5	19	13	6.4	1.8
4.6	51	30	15	3.1
4.7	3.8	2.2	1.0	0.35
4.8	4.8	2.4	1.6	0.38
4.9	3.6	2.2	1.3	0.33
5.1	4.5	2.9	1.6	0.36
5.2	6.2	4.3	2.3	0.57
5.3	5.9	3.8	1.7	0.37
5.4	40	27	13	3.0
5.5	41	23	13	2.8

5.6	44	26	15	3.3
5.7	3.9	2.3	1.3	0.30
5.8	4.7	3.0	1.6	0.34
5.9	3.4	2.0	1.3	0.33
Right side	39	26	13	2.6
Left side	54	32	20	3.5

Table 4.5: Absorbed dose [mGy] from TLD-100 measurements on the surface of the abdominal phantom. The absorbed doses are received for one CBCT-rotation with the EVAR protocols on Artis Q. Position 1 and 5 represent the anterior and posterior projection, and position 3 and 7 the left and right projection, respectively.

	Absorbed dose [mGy] of TLD on Artis Q			
	CBCT protocol			
TLD position	**6sDCT Body**	**5sDCT Body Care**	**5sDR Body**	**5sDR Body Care**
1	15	8.5	4.7	1.2
2	41	23	15	3.0
3	66	39	22	4.4
4	64	43	24	5.0
5	64	37	23	5.3
6	58	37	20	4.0
7	51	35	18	3.6
8	22	13	8.6	1.7

4.2 Scoliosis

4.2.1 Protocol Comparison

4.2.1.1 Radiation dose

Figure 4.9 presents the effective dose [mSv] for the scoliosis protocols on *Artis Pheno* and *Artis Zeego*. The protocol group 1 represents the normal dose protocols, *5sRygg Normal dose 3D* and *CT Normal dose 5s R15P85*, and group 2 the low dose protocols, *5sRygg Low dose 3D* and *CT Low dose 4s R15P85*, on *Artis Pheno* and *Artis Zeego*, respectively. With the protocols from group 1 a higher effective dose was received compared to group 2. The highest effective dose was received from the protocol *CT Normal dose 5s R30P8* on *Artis Zeego*.

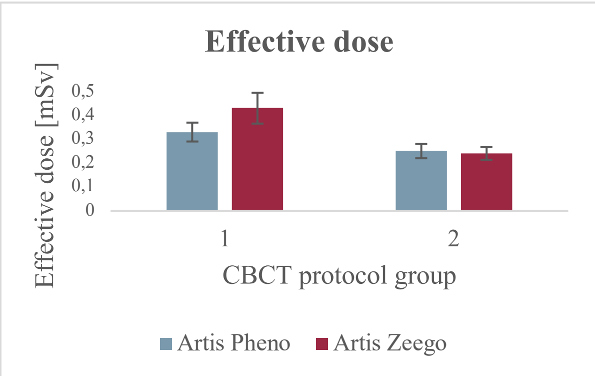

Figure 4.9: Effective dose [mSv]] for the CBCT scoliosis protocols used on Artis Pheno and Artis Zeego, using the abdominal phantom. Group 1: 5sRygg Normal dose 3D and CT Normal dose 5s R15P85, group 2: 5sRygg Low dose 3D and CT Low dose 4s R15P85. The error bars indicate the uncertainties in calculations with PCXMX20Rotation.

In Appendix B, Table B.12 and B.13, the radiation doses, DAP [$Gycm^2$], DAP per detector area, DAP/A [mGy], IAK in the reference point, $D_{skin,DICOM}$ [mGy], and absorbed dose rate, $\dot{D}$ [mGy/s], E [mSv], and absorbed doses, $D_{skin,PCXMC}$, D_{ABM}, Dcolon, $D_{kidneys}$, $D_{ovaries}$ and D_{SI} [mGy] are presented. On *Artis Pheno* and *Artis Zeego* the radiation dose was decreased, for all dose quantities, using the low radiation dose CBCT scoliosis protocols, group 2. The relative radiation dose, for all radiation dose quantities, between the normal and low dose protocols, group 1 and 2, are presented in Appendix B, Table B.14, and the quotient of effective dose between the protocols is a factor 1.3 and 1.8, on *Artis Pheno* and *Artis Zeego*, respectively.

In Appendix B, Table B.15, the percentage difference in radiation dose between the modalities are presented. The normal and low radiation dose protocol on *Artis Pheno* were compared to the normal and low radiation dose on *Artis Zeego*. It was shown that DAP, $D_{skin,DICOM}$, and $\dot{D}$ on *Artis Pheno* was higher than on *Artis Zeego* (note that the protocols on *Artis Zeego* has the filtration 0.9 mmCu and on *Artis Pheno* 0.1 mmCu). Meanwhile, the effective dose and absorbed organ doses were lower for the normal dose protocols on *Artis Pheno* compared to *Artis Zeego*, but higher for the low dose protocols. Also, note that the protocol *CT Low dose 4s R15P85* (*Artis Zeego*) takes a larger angle step than *5sRygg Low dose 3D* (*Artis Pheno*).

4.2.1.2 Image quality

In Table 4.6 the number of line pairs per cm is shown. On both protocols from *Artis Pheno* and for *Artis Zeego*, *CT Normal dose 5s R15P85*, a higher number of line pairs per cm was seen compared to *CT Low dose 4s R15P85* (*Artis Zeego*).

Table 4.6: Number of line pairs per cm for each scoliosis protocol.

Modality	Protocol	Line pairs per cm (lp/cm)
Artis Pheno	5sRygg Normal dose 3D	8
	5sRygg Low Dose 3D	8
Artis Zeego	CT Normal dose 5s R15P85	7
	CT Low dose 4s R15P85	4

4.2.2 CT

In Figure 4.10 the effective dose [mSv] for the protocols used in CT-measurement with different settings is presented. When using the automatic setting (higher tube current), the effective dose increased. When the CBCT scan range was used instead of the CT scan range, the scan range decreased and also the DLP, effective dose and equivalent doses, as expected. In Appendix B, Table B.16, the radiation dose quantities, $CTDI_{vol}$, DLP, effective dose and equivalent organ doses are presented, for all CT scoliosis protocols and settings.

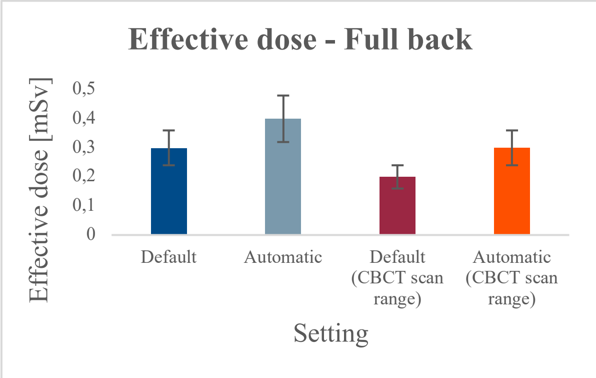

Figure 4.10: Effective dose [mSv] for the CT scoliosis protocols, with different settings, using the abdominal phantom. The error bars indicate the uncertainties in calculations with CT-Expo.

4.2.3 CBCT vs CT

In Table 4.7 the effective dose quotient between the scoliosis protocols from CBCT and CT, are presented. When using the normal dose protocols the effective dose received from the CBCT was higher, up to a factor 2.1, than that from the CT, except for *4sRygg Normal dose 3D* (*Artis Pheno*) compared to *Full back Automatic*. For the two low dose CBCT protocols, the effective dose received from the CBCT was a factor 0.59-0.84 lower than from the CT scan, except for the CT settings *Full back default* with a scan range the same as the CBCT, which gave a factor 1.2-1.3 higher effective dose than the low dose CBCT.

Table 4.7: Relative values between the effective doses for the CBCT and CT scoliosis protocols, using the abdominal phantom.

		CBCT scoliosis protocol			
CT scoliosis protocol	**Setting**	**4sRygg Normal dose 3D**	**CT Normal dose 5s R15P85**	**4sRygg Low dose 3D**	**CT Low dose 4s R15P85**
Full back	**Default**	1.1	1.4	0.84	0.79
	Automatic	0.82	1.1	0.63	0.59
	Default (CBCT scan range)	1.6	2.1	1.3	1.2
	Automatic (CBCT scan range)	1.1	1.4	0.84	0.79

4.2.4 Tube output

For the CBCT scoliosis protocols on *Artis Pheno*, the tube current-exposure time product [mAs] was not changing much during the rotation, as shown in Figure 4.11, which was representative for both protocols. A slight decrease in tube current-exposure time product was seen in the posterior-anterior direction. For the protocols on *Artis Zeego*, a larger change was seen in the tube current-exposure time product over the projections, see Figure 4.12. As for the scoliosis protocols on *Artis Pheno*, the tube current-exposure time product was decreased in the posterior-anterior direction (-30° to 30°).

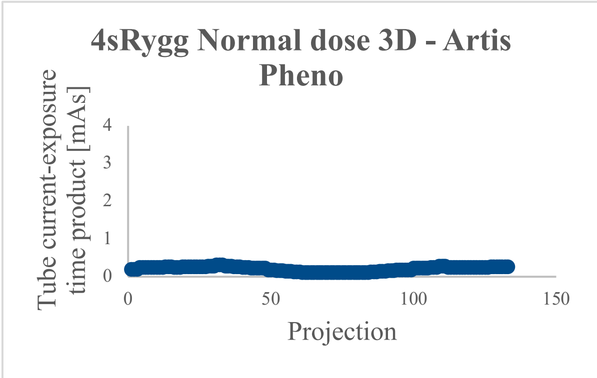

Figure 4.11: Tube current-exposure time product [mAs] at different projections, for the CBCT scoliosis protocol 4sRygg Normal dose 3D on Artis Pheno, using the abdominal phantom.

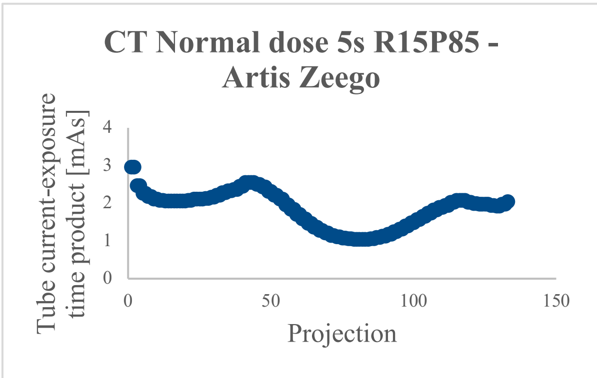

Figure 4.12: Tube current-exposure time product [mAs] at different projections, for the CBCT scoliosis protocol CT Normal dose 5s R15P85, on Artis Zeego, using the abdominal phantom.

4.2.5 Radiation dose to personnel

Figures 4.13 and 4.14 present the estimated radiation doses to the dosimeter at a personnel position using the scoliosis protocols on *Artis Pheno* and *Artis Zeego*, respectively. At a longer distance to the center of the patient, the radiation dose decreased. As expected, the estimated personnel radiation dose was decreased when using the low dose protocols, on *Artis Pheno* and *Artis Zeego*, respectively.

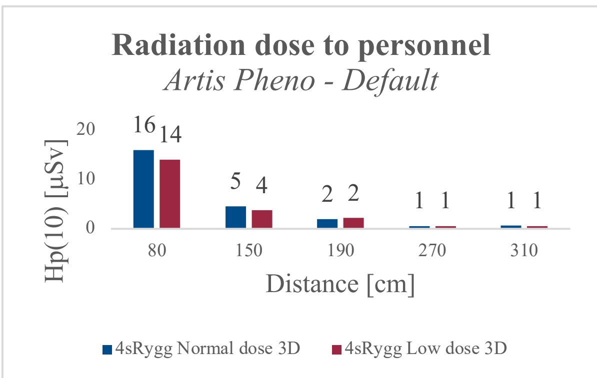

Figure 4.13: Estimated radiation dose, $H_p(10)$ [μSv], to personnel during CBCT, with the protocols for scoliosis on Artis Pheno, at different distances from the center of the patient.

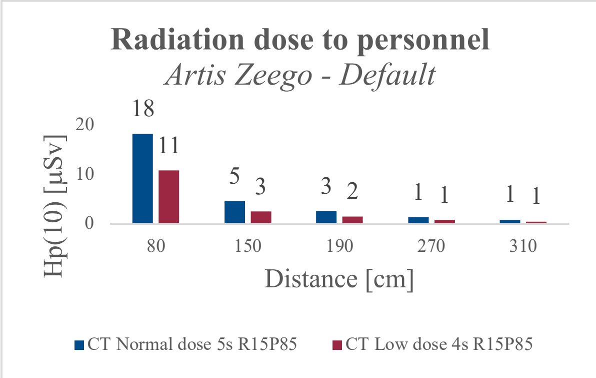

Figure 4.14: Estimated radiation dose, $H_p(10)$ [µSv], to personnel during CBCT with, the protocols for scoliosis on Artis Zeego, at different distances from the center of the patient.

5 Discussion

In this project radiation doses and image quality for EVAR and scoliosis procedures have been investigated. Radiation doses from CBCT in interventional fluoroscopy and OR have also been compared to the radiation doses received with CT. The project was performed to receive more knowledge about CBCT, why it is used during different procedures and to evaluate the tube output and doses received. The EVAR procedures were chosen to be investigated because they are high in radiation dose to patients and sometimes make use of CBCT, one time or several times, during surgery. In liver procedures, the radiation doses are even higher, and CBCT is performed more often. However, these patients are often late in their disease, elderly and are also often treated palliatively, which makes it more entitled to give these patient's a higher radiation dose. EVAR patients are, though, compared to the liver patients, not as sick. The mean percentage dose received from CBCT during EVAR procedures, where CBCT has been used, is 22% (6.8-72%, n=24) (data not shown). Scoliosis patients, who need to undergo surgery, are often young girls. This is one important reason to reduce the radiation dose. Also, to diagnose scoliosis and for follow-up, x-rays are used, and these patients are therefore undergoing several x-ray examinations. The scoliosis protocols were therefore chosen to be evaluated because of the need to keep the radiation dose low. The radiation doses to patients, received from both CBCT and CT imaging, are relatively high. Surgeons have a good knowledge of radiation doses to patients undergoing a CT, however, when it comes to CBCT the knowledge decreases somewhat. This results in CT being an appropriate modality to compare the radiation doses received from CBCT. It is very important to be aware of the radiation doses during CBCT, since a CBCT is easier performed in an OR during surgery without much time to consider the justification.

Two phantoms were used for radiation dose measurements, PMMA and abdominal phantom. The PMMA phantom is not constructed as a patient. However, it is good for relative measurements and for evaluation of how the radiation dose is distributed throughout the phantom. The abdominal phantom was used to represent a normal man. Comparisons of DAP, for EVAR procedures, between the abdominal phantom and real patients have been made (data not shown), which shows that the abdominal phantom is thinner than a normal person. If a different phantom size had been used, it is difficult to predict the result. One would think that the relative value between different protocols would be unchanged for different phantom sizes, however, the automatic exposure control will be changed.

Initially, the interest in collimation and zoom was weather it was even possible to use during CBCT. Since it was possible, this led to several measurements using different settings for collimation and zoom. The protocols used for evaluation of radiation dose during EVAR procedures are named differently on each of the modalities. These were, though, chosen to correspond to each other but there are some differences between the modalities and protocols. The FDD on *Artis Pheno* is 130 cm compared to 120 cm on *Artis Q* and *Artis Zeego*. The detector size and FRD, is still equal between the modalities, which means that the field entering the patient (or phantom) on *Artis Pheno* is smaller. With a longer FDD, the system needs to produce more radiation to compensate for the longer distance. However, because the field entering the patient is smaller, the two parameters cancel each other out, except for IAK in the reference point which increases, as seen in Appendix B, Table B.1-B.3. Another difference between the modalities is the zoom in the default setting. On *Artis Pheno* it is 50 cm while on *Artis Q* and *Artis Zeego* it is 48 cm. The zoom was available in discrete steps and the choice was displayed on the screen. To collimate, a joystick was moved and lines on the screen showed the collimation, but no numbers displayed the image size. The same collimation was tried to be reproduced by setting the collimation lines at the same height at different markers, which were fixed on the screen. Thus, there was a difference using collimation 1 (8% smaller radiation field on *Artis Q* and *Artis Zeego*, compared to *Artis Pheno*), but no consideration was taken to this. The scoliosis protocols were chosen in the same way as the EVAR protocols, so that they would correspond to each other, on the two modalities. However, the protocols used in the scoliosis evaluation had a bigger difference between them. The protocols on *Artis Pheno* had the filtration 0.1 mmCu and on *Artis Zeego* 0.9 mmCu. The dose for the low dose protocol on *Artis Pheno* (*4sRygg Low dose 3D*) was set to 0.08 µGy/f and on *Artis Zeego* (*CT Low dose 4s*

R15P85) to 0.1 μGy/f. For the protocols *4sRygg Normal dose 3D* and *CT Normal dose 5s R15P85*, on *Artis Pheno* and *Artis Zeego*, respectively, the dose was set to 0.1 μGy/f. The 3D angle step for both of the scoliosis protocols on *Artis Pheno* and *CT Normal dose 5s R15P85* on *Artis Zeego* was 1.5°/f, but for *CT Low dose 4s R15P85* on *Artis Zeego* it was 3.0 °/f. and the FDD was 130 cm compared to 120 cm on *Artis Pheno* and *Artis Zeego*, respectively. On the modalities, there was one additional scoliosis protocol available, a high dose protocol. However, this is not used since the patients often are young girls and do not require a high dose protocol. Due to this, the high dose protocol was not evaluated, and maybe this protocol should be removed since it is not used. Also, no other settings, except the default settings, were evaluated for the scoliosis protocols. Collimation and zoom are not used during scoliosis surgeries, because the full detector size is needed to contain all the pedicle screws. In some cases, even additional CBCT is needed to be able to include all the pedicle screws. Due to time constraints, measurements with pedicle screws were not performed. When centering the abdominal phantom, markers on the phantom were used to ensure that the centering became the same on all modalities. On *Artis Q* and *Artis Pheno* lasers and fluoroscopy were used to ensure that the centering was correct. On *Artis Zeego*, no lasers were available. However, the measurements on *Artis Zeego* were performed last and since no lasers were available on *Artis Zeego*, images from *Artis Q* and *Artis Pheno* in combination with fluoroscopy were used to make sure that the centering became the same.

Effective doses and absorbed organ doses received from CBCT and CT examinations have been compared. The effective dose should not be calculated for individual patients, since it is a risk quantity suitable for a population, and uses mean values for a reference person. However, since the same phantom is used for all measurements and the radiation fields are approximately the same between the modalities, calculations of effective dose for CBCT and CT is a way of comparing the different modalities. One difference in the calculations with PCXMC20Rotation and CT-Expo is the patient size. In PCXMC20Rotation the patient size is set to 175 cm and 73 kg and in CT-Expo 170 cm and 70 kg. In PCXMC20Rotation the height and weight could be chosen in any way, but in CT-Expo it was set to 170 cm and 70 kg when using an adult male as the setting choice. If a comparison, with PCXMC20Rotation, is performed with the parameter values on *Artis Pheno*, using the default settings, but with two different patient sizes, an increase in effective dose is given for the size 170 cm and 70 kg, with 5.7% ± 0.36%. This entails that the effective dose for the CT calculations is higher than CBCT, because of the difference in patient size, though, this does not significantly affect the result. In CT-Expo equivalent doses [mSv] was received. However, the equivalent dose can easily be converted to absorbed dose [Gy], since the x-ray modality uses photons which have the radiation weighting factor, w_R=1, see Eq. (3). The absorbed organ doses evaluated were in the radiation field, and therefore also receiving the highest absorbed dose. In the effective dose calculations with CT-Expo, the patient was chosen as an adult male, and no equivalent dose of the ovaries was received, in contrast to the PCXMC20Rotation calculations. The patient height and weight used for all of the effective dose and absorbed organ dose calculations were, as previously mentioned, 175 cm and 73 kg. Meanwhile, for the scoliosis procedures, normally the patients are young girls and 175 cm and 73 kg is therefore an overestimate of the patient size. However, the phantom used during measurements is also an overestimate, which might have affected the tube current-exposure time product to be increased compared to for a normal patient. It is therefore difficult to predict if the absorbed dose to the patient is over or underestimated and no consideration to this was taken.

No repeated measurements were made, except for the default settings on *Artis Q* and *Artis Pheno*. This led to that the statistical significance could not be decided for all different settings and modalities (*Artis Zeego*). The error in DAP, IAK in the reference point, absorbed dose rate, $CTDI_{vol}$, DLP is estimated to be ±10%. The same phantom and positioning were used for all measurements on all modalities, and the input data were collected from the modalities to make sure that the calculation error was minimized.

When performing a CBCT, the radiation field does not cover the whole patient at all angles for the EVAR protocols. In the longitudinal direction (anterior-posterior direction) of the phantom, the radiation field was always inside the phantom boundaries. However, laterally (right-left direction), 20% of the radiation field size ended up outside the phantom on *Artis Q* and *Artis Zeego* (FDD=120 cm). On *Artis Pheno* (FDD=130) only 3% of the radiation field ended up outside the patient in the lateral direction. Because of this, the radiation dose quantities received were overestimated, but less for *Artis Pheno*, except when calculating effective dose and absorbed organ doses with PCXMC20Rotation. For the settings default, collimation 1 and 2, this effect was present. However, for zoom 42 and 32, the whole radiation field covered the phantom and therefore, did not overestimate the radiation dose. Compared to the default setting, the radiation dose, DAP, effective dose and absorbed organ doses decreased when using collimation and zoom, see Appendix B, Table B.1, B.2 and B.3. When using collimation, the radiation field size was decreased and a smaller part of the phantom was covered. DAP/A and IAK in the reference point, $D_{skin,DICOM}$, and absorbed dose rate, $\dot{D}$, is, though, increased. This may depend on, when the field size decreases, a smaller part of scattered radiation hits the detector, resulting in a slightly increase in tube output, to compensate for the loss of scattered radiation to the detector leading to an increased DAP/A, $D_{skin,DICOM}$ and $\dot{D}$. DAP, effective dose and absorbed organ doses are, though, decreased because the increase of tube output is smaller than the decrease in field size. When using zoom on a digital detector, the output of the tube increased to compensate for the noise impression, which increases with zoom. This lead to an increase, compared to the default setting, in DAP/A, $D_{skin,DICOM}$ and $\dot{D}$, which was seen for all protocols on all modalities (Appendix B, Table B1-B3). However, the radiation field entering the patient was decreased when zoom was used. DAP, effective dose and absorbed organ doses, were also decreased, and one reason for this is the smaller radiation field entering the patient. The field size also affects the absorbed organ doses. When the field size is decreased, some organs might end up outside the field and the absorbed dose decrease sharply. As an average factor for all protocols and modalities, compared to the default value, DAP/A was increased with a factor 1.1, 1.3, 1.6 and 5.0 $D_{skin,DICOM}$ with a factor 1.1, 1.4, 1.2 and 2.2 and $\dot{D}$ with a factor 1.1, 1.4, 1.2 and 2.1, for collimation 1, collimation 2, zoom 42 and zoom 32, respectively. For the EVAR procedures, it is important to keep the skin dose low since this is a procedure that risk to cause skin injuries. This should be considered when choosing to use zoom 32, since this gave the highest increase of DAP/A, IAK in reference point and absorbed dose rate, even if the DAP and effective dose was decreasing. The effective dose received during CBCT with the scoliosis protocols was much lower than for EVAR procedures since the scoliosis protocols used a higher tube voltage and a lower dose per frame. A decrease was also seen when using the low dose protocols (*5sRygg Low dose 3D* and *CT Low dose 4s R15P85)* compared to the normal dose protocols (*5sRygg Normal dose 3D* and *CT Normal dose 5s R15P85)*. Normally the low dose protocol is used during scoliosis surgeries. The tube current-exposure time product was higher on *Artis Zeego* for both scoliosis protocols but a 0.9 mmCu filtration was used for the protocols on *Artis Zeego* which results in more attenuation of the low-energy photons. Therefore, the tube current-exposure time product was increased. The quotient between the high and low dose protocol on each modality was quite different on *Artis Pheno* and *Artis Zeego* (a factor 1.3 and 1.8, respectively). The difference on *Artis* Zeego was seen because the protocol *CT Low dose 4s R15P85* takes a larger angle step than *CT Normal dose 5s R15P85*. The effect on the radiation dose, because of the larger angle step, was also seen when comparing the low dose protocols between the modalities. When the normal dose protocols were compared between the modalities, a decrease in effective dose and absorbed organ doses was seen on *Artis Pheno*. One reason for this might be the smaller radiation field entering the patient on *Artis Pheno* (FDD=130 cm). Moreover, during surgery, the scoliosis patient is not in a supine position. When effective dose and absorbed organ doses were calculated, the phantom in PCXMC20Rotation should be rotated 180°, but this was not done. The error in effective dose and absorbed organ, because of this, was estimated to be minimally.

The image quality was investigated using the high-resolution module in Catphan. This section was chosen to be investigated since contrast agents are used to enhance visualization of vessels during EVAR procedures. Surgeons also want a good low contrast sensitivity, and it would be desirable to evaluate this. However, an attempt was tried to do this on one protocol. The low contrast section in Catphan was found, but the low contrast targets were barely seen at all, therefore no evaluation was made. The line pairs per cm seen, when evaluating the image quality for EVAR and scoliosis protocols were the same on all modalities, except for the protocol *CT Low dose 4s R15P85* on *Artis Zeego* that had a lower spatial resolution. The decrease in spatial resolution might be because of the large angle steps compared to the other protocols. For the two high radiation dose protocols on each modality, *Artis Q*, *Pheno* and *Zeego*, the resolution was set to *low* in the protocol settings, and for the two low radiation dose protocols to *medium* (Table A.1, A.2 and A.3). Intuitively it is thought that the high dose radiation protocol would lead to a better high-resolution. However, the pixels are binned with the resolution *low*, which leads to a decrease in high-resolution. The pixels are binned in the high radiation dose protocols to decrease the noise in the images.

For the CBCT and CT measurements, no contrast agent was used. Amato *et al* presents that the use of a contrast agent in CT results in an increase of radiation dose in several organs [35]. With this knowledge is was important to have in mind that the radiation dose increase even further when using a contrast agent, compared to exposures without contrast agent. There are three different CT protocols used for EVAR. *Aorta before EVAR* is performed before the surgery and covers the abdominal area. About a month after the surgery, a post-op CT is performed. Two CT protocols are combined, one with and one without contrast agent (*EVAR without contrast + abdominal aorta after EVAR*), which resulted in a doubled effective dose compared to *Aorta before EVAR*. If there is any reason to suspect leakage, a further scan can be performed, called *Late series EVAR*. With this protocol, only the stent is scanned. On the CT used for the measurements, the tube voltage was 120 kV. On other CT scanners, also used for EVAR examinations, the tube voltage is set to 100 kV. With this knowledge, both 100 and 120 kV were used. For CT scoliosis one protocol was used, *Full back*. For scoliosis patients the scan range is normally larger than the one used with the measurements on the abdominal phantom. The abdominal phantom is not long enough to cover the full scan length of a real patient. Using the patient real scan length might, therefore, result in a larger radiation dose for both CT and CBCT. The abdominal phantom used was bigger in size than the normal scoliosis patient, which often is young girls as previously mentioned. When the first scan was performed, the CT indicated that the tube current should be increased, which also indicates that the phantom used is larger than a normal scoliosis patient. This resulted in one scan with the default tube current and one with the larger (automatic) tube current. Also, calculations with the CBCT scan range was used, as for the CT EVAR protocols. To be able to compare the CT scans with the CBCT, the same scan range was used when calculating the quotient between the effective doses. However, in the CT scans a longer scan range is normally used for all the EVAR and scoliosis CT protocols, except for *Late series EVAR*, as described above. $CTDI_{vol}$ for *Aorta before EVAR, EVAR without contrast* and *Abdominal aorta after EVAR* was the same when using the same settings, see Appendix B, Table B.15. The *Late series EVAR* had a decreased $CTDI_{vol}$, compared to the other protocols, and therefore a lower effective dose was received when using the same settings. When the tube voltage was changed from 120 kV to 100 kV the effective dose was increased for all protocols except *Late series EVAR*. With the change in tube voltage, the tube current was automatically increased. With a lower tube voltage, the photons will interact more often and an increase in tube current is needed so that the detector gets enough signal. This resulted in an increased effective dose. For the *Late series EVAR*, the tube current was not increased as much as for the other protocols, which may be a reason for the small decrease in effective dose. CT scans have been performed with a scan range covering the abdominal phantom. On a real patient a longer scan range may be used since the abdominal phantom is not a full-size patient. However, it would be interesting to know if longer scan range always is needed for the CT scan, or if smaller scan rages can be used in some cases. If a longer scan range is used this may result in a more equal effective dose between the CT and CBCT, for some protocols. For example, if instead of a CT scan, a CBCT is used because this CBCT protocol gives a lower effective dose. It might be that the CBCT field size does not cover the whole area needed to receive the same information as the CT, and an additional CBCT must be performed, raising the radiation dose above CT. On the other hand, on a CT, the scan range can be set to cover the whole patient. While performing a CBCT several rotations may be needed to cover the whole area. However, when the same scan range was compared, the two high dose CBCT EVAR protocols (group 1 and 2), on all modalities, gave a higher effective dose than the CT protocols (except when *EVAR without contrast + abdominal aorta after*

EVAR was used since these are two CT scans). The low radiation dose CBCT EVAR protocols on all modalities (*5sDR Body Care*, *4sDR Body Care* and *5sDR Body Care R30,* group 4), gave a lower effective dose than the CT scan. Maybe, if the same information can be received as when CT is used, or sufficiently information, the CT may be replaced with a CBCT to receive a lower effective dose. With the scoliosis CT protocols, *Full back automatic* (increased tube current), the effective dose became higher since the tube current increased and the other parameters (such as tube voltage) was unchanged. If the same scan range on CT and CBCT was compared it was for the normal dose CBCT protocols better to choose CT to receive a lower effective dose. However, for the low dose CBCT protocols, the effective dose was almost equal using the CT (automatic). With a real scoliosis patient, which normally is thinner than the abdominal phantom, the tube current should not have to be increased, which results in a lower effective dose on CT than on CBCT.

In most cases, fluoroscopy is used when performing 2D-3D-fusion, with a few pulses, frontal and lateral. Exposures are rarely used, though, sometimes at specific occasion it may be necessary. For instance, if the patient is overweight and has its arms along the body. Between surgeons, there is no difference in how the fusion is performed (*Operator at intervention 1, Sahlgrenska University Hospital, personal communication, Nov 11, 2018)*. When comparing 2D-3D fusion with 3D-3D fusion it is seen that 2D-3D fusion should be used to receive a lower radiation dose. However, the matching between the two images might be better using 3D-3D fusion, since 2D-3D fusion does not focus on the aorta and only the bones, while registering the two image data sets together [9].

Tube current-exposure time product was decreased for all protocols on all modalities in the posterior-anterior direction. This was the direction where the phantom was thinnest, and the tube current-exposure time product was therefore decreased. For some protocols, the tube voltage was changed during the rotation. When the tube voltage was increased, it is seen that the tube current-exposure time product was decreased. These work in opposite directions to keep the radiation dose at a preferable level. Three protocols that stood out when comparing the tube current-exposure time product and tube voltage were *5sDCT Body L*, *4sDCT Body Care L* and *4sDR Body L* on *Artis Pheno* using zoom 32. The radiation doses, DAP, $D_{skin,DICOM}$, $\dot{D}$, effective dose and absorbed organ doses did not, though, stand out. When comparing the same protocols on the different modalities a slight difference was seen for some radiation dose quantities, not significant. The modalities rotated in the same angle interval but had different start and end positions (see Figure 3.7). This entails that the absorbed organ doses may differ on the modalities. For some protocols the tube current-exposure time product was higher on a lower dose protocol, see Figure 4.5b and c and Figure 4.7b and c. However, the radiation dose dis not significantly increase because of this, since different angle steps were used for the protocols, see Appendix B, Table B.1-B.3.

For the measurements of radiation dose to a personnel dosimeter position, real-time dosimetry system was used. These were placed at different distances from the center of the phantom. On the different modalities, the dosimeters were placed in the same way, but it was quite difficult to get the same placement of the dosimeters on all modalities. This resulted in that no direct comparison between the radiation dose to a personnel position on different modalities was made. It is clearly shown that an increased distance to the patient center results in a lower personal radiation dose, which is not a surprise since the intensity of the radiation beam is inversely proportional to the distance in square. By using a protocol that gives a lower radiation dose, did not only result in a lower radiation dose to the patient, but also to the personnel position. When collimation is used, the radiation field and therefore the scattered radiation is decreased, which leads to a decrease in measured personnel radiation dose. A lower estimated personnel radiation doses was also obtained by using zoom, which correlates with the measurements and calculations of DAP, effective dose and absorbed organ doses. The tube current-exposure time product is, though, increased which should lead to a higher estimated personnel radiation dose, but this was not the case. One reason for the decrease in the estimated personnel radiation dose, while zooming, may be that the smaller radiation field results in less scattered radiation, which overcomes the increase in tube current-exposure time product. Also, the scattered radiation must go through a larger part of the phantom which instead leads to that the photons are absorbed. During surgeries, when CBCT is performed, personnel normally is placed behind radiation shields several meters from the patient and uses radiation protection aprons. This are important tools to keep the radiation dose to personnel as low as possible. The radiation dose to a personnel position is not different comparing the two scoliosis protocols on *Artis Pheno*. On *Artis Zeego* the difference is bigger since the protocol *CT Low dose 4s R15P85* uses a larger angle step. However, compared to the EVAR protocols the estimated personnel radiation dose is much lower. For the scoliosis procedures, the surgeons normally do not use radiation aprons but is placed behind a radiation shield during the CBCT.

The radiation quality used for the calibration of TLD was RQA7. This represents measurements behind the patient and additional filtration is made with aluminum [32]. RQA7 uses the tube voltage 90 kV, and was chosen since that is the tube voltage used for all of the EVAR protocols (see Appendix A, Table A.1-A.3). When the tube voltage on the x-ray system was measured, the output tube voltage was lower than it was set to be. Therefore, a tube voltage of 96 kV was set on the system to receive a peak tube voltage of 92 kV, which was the closest to 90 kV possible. To determine the absorbed dose of the TLDs, the mean tube voltage of the x-ray spectrum with RQA7 was determined. In the simulation of the x-ray spectrum, the relative voltage ripple was set to zero. This gives a higher mean energy of the spectrum than, for example, when the ripple is set to one (60.7 kV compared to 58.0 kV). In the real case, the ripple is higher than zero, but this error is estimated to be small in consideration to the total error. To determine the absorbed dose in PMMA the quotient of the mass energy-absorption coefficient between PMMA and air was used. The mass energy-absorption coefficient is specific for different photon energies, and the mean tube voltage 60.7 kV was used for calculations. The tube output consists of a spectrum of energies, which makes the calculations of the absorbed dose inaccurate. To estimate a correct absorbed dose, each of the energies in the x-ray spectrum should be taken into consideration, though, this has not been done. When TLD measurements free in air, to receive the BSF, were performed, the TLDs were placed in small holes in a PMMA slice. Since this is not a free in air measurement, it means that the backscatter is higher than in a completely free in air measurement. This results in a measured BSF that is smaller than the actual BSF, which in the end may result in an underestimate of the absorbed dose. This might also lead to an absorbed dose in the PMMA closer to the IAK in reference point (see Appendix B, Table B.1-B.3). The absorbed dose to the PMMA phantom is thus determined by several different measurements and estimates. To correctly determine the absorbed dose, calculations with the whole x-ray energy spectrum should be performed, and measurements of the BSF with completely free in air measurements should be made. The estimated error in the calculations of absorbed dose in PMMA is 40%. However, the estimated absorbed dose received by the TLDs gives a hint of its actual absorbed dose and when the protocols are compared relatively the calibration factor does not affect the result. Also, the positions in the PMMA phantom, receiving the highest and lowest absorbed doses, can be decided.

When the absorbed dose during a CBCT was determined, all TLDs were placed at different depths and positions at each depth. When the rotation started some of the TLDs were close to the x-ray tube, but at the end of the rotation they were far away from the x-ray tube. The TLDs will, therefore, get hit by different x-ray spectrums throughout the rotation, and have different scattering situations because of the difference in material thickness around the TLDs. Determination of the correct absorbed dose for each TLD position would be to decide a calibration factor unique for each TLD position. However, as previously mentioned, the difference in absorbed dose at different positions in the phantom can still be estimated, and relative calculations can be made. The same limitations are also present when measuring TLD absorbed doses with the abdominal phantom. The TLDs will get hit at different angles and with a change of the x-ray energy spectrum.

The first TLD measurement was made to decide how many rotations were required to get a signal from the TLDs (data not shown). The integral radiation dose from three, five and seven rotations were collected, and the result showed that only one rotation was needed. Before the CBCT could be performed a short time of fluoroscopy was needed so that the modality could adjust output parameters. At this fluoroscopy 0.5 p/s was used to minimize the radiation dose to the TLDs before the CBCT. When the TLDs were read out, it was found that some of the glow curves were shifted to the right. Because of this, another readout was performed, and some of the TLDs still contained charge (0-5% of the total absorbed dose). With this knowledge, no further TLD measurements were made. One reason for the shifted glow curves may have been that some of the TLDs received its maximum radiation dose in the measurements when deciding the number of rotations. However, it is unlikely that this is the case when further investigations have been made. The investigation of the shifted glow curves is still in progress.

In the PMMA phantom, the TLD positions 4, 5 and 6 on each plane were the ones receiving the highest absorbed dose. At these positions the radiation scatter was higher than for the positions closer to the edge. For the TLDs on the phantom sides, the left side received the highest absorbed dose for all protocols. On *Artis Q* the x-ray tube was moving 200° underneath the patient (as seen in Figure 3.7a), with 100° equally distributed between the right and left side. This entails that the absorbed dose should be equal on both the right and left side dosimeter. The output of the x-ray tube might have changed from the right to the left side of the phantom since the absorbed dose is increased. However, Figure 4.5a-d, showed that the change in tube current-exposure time product and tube voltage, did not differ between the right and left side. Another reason for the difference between the right and left side might be explained by an offset of the lasers, used for centering, that may have caused a shorter distance between the x-ray tube and the left side TLD. The same pattern was seen in the other planes, where position 6 received the highest absorbed dose. Also, in the TLD measurements with the abdominal phantom, the left side TLD was receiving a higher absorbed dose (up to a factor 1.3).

The relative difference in effective dose between the protocols on each modality was a factor 16, 9.0 and 4.8. How do the interventional operators choose which protocol to use? Is it entitled to use, for example, the highest dose protocol since the effective dose was a factor 16 higher than the lowest CBCT EVAR protocol? The highest dose protocols gave an effective dose that is three times higher than a CT scan with the same scan range. Is it entitled to use a CBCT in that case, or should a CT examination be used instead, if the same information can be received? In the OR, were EVAR is performed, there are instructions on how the protocols can be chosen. The high radiation dose protocols, with low resolution, is mainly used when a decrease in noise is needed. The low radiation dose protocols are better when looking at high contrast differences, as during scoliosis procedures. Further studies are required to determine how different protocols are used and if the highest dose protocols are needed.

The names of the CBCT protocols are a bit confusing. There are two EVAR protocols called *Care*. *Care* is used for protocols giving a low radiation dose. One of these two *Care* protocols gives the lowest effective dose, and the other, the second highest, making it very deceptive to use the name *Care*. The only part in the name that separates the protocols (*5sDR Body Care* and *5sDCT Body Care*) is DR and DCT. Without having this explained beforehand, it is hard to know that DR gives a lower radiation dose than DCT. Moreover, when the protocols *5sDR Body* and *5sDCT Body Care* are compared, how is it known than *5sDCT Body Care* gives a larger radiation dose, even if *Care* is used in the name? To become more confident, in which protocol the highest radiation dose is produced, it may be considered to rename the protocols, although most interventional operators are experienced and used to these names. They might also have the knowledge to tell them apart when it comes to radiation dose. However, for the scoliosis protocols, the name contains *Low*, *Normal* or *High*. This naming reminds of the ones used for fluoroscopy protocols, and instantly gives a hint of which one of the protocols gives the highest radiation dose. Three of the protocols on *Artis Pheno* have an L in them, which implies *landscape* mode. Meanwhile, on the protocol *4sDR Body Care,* on *Artis Pheno,* the name contains no L, but *landscape* mode is still used. On *Artis Zeego*, the protocols have R30 and R15P85, which implies the table rotation. For the CBCT EVAR protocols, this project has led to that the protocol names are to be changed, to become more confident in which protocols the highest radiation dose is produced and how to choose protocol for different situations.

Future studies of CBCT might be needed to evaluate the radiation dose and image quality on real patients and to include a more profound evaluation of the image quality. Furthermore, studies involving other types of procedures using CBCT, for instance, neurology procedures and other procedures used in vascular surgery.

6 Conclusion

In this project radiation doses from CBCT with different protocols, used for EVAR and scoliosis procedures, on three different modalities, *Artis Q*, *Pheno* and *Zeego*, have been investigated. The radiation doses were evaluated by measurements with TLD, collecting radiation dose values from the modalities, such as DAP, IAK in the reference point (received from the DICOM data) and absorbed dose rate, and also by calculating effective doses and absorbed organ doses with PCXMC20Rotation and CT-Expo. Furthermore, the effective doses from CBCT were also compared with effective doses received at CT, with different CT protocols used for EVAR and scoliosis. The image quality was evaluated using the high-resolution module in *Catphan*. DAP received when performing 2D-3D-fusion was compared to 3D-3D-fusion. Also, personnel radiation dose estimate was evaluated for different distances to the patient for all protocols and settings.

The maximum relative effective dose, between the four EVAR protocols, on all modalities, are 16 for the highest dose protocol, 9.0 for the second highest protocol and 4.8 for the second lowest protocol, compared to the low radiation dose protocol. Between the two scoliosis protocols, the relative effective dose value is 1.3 and 1.8 on *Artis Pheno* and *Artis Zeego*, respectively. Collimation is a good tool to reduce the radiation dose to the patient. Also, using zoom reduces DAP and effective dose, though, IAK in the reference point increases. There is no difference in spatial resolution between the protocols on the different modalities, except for the scoliosis CBCT protocol, *CT Low dose 4s R15P85*, wich has a lower spatial resolution. For the highest dose protocols, CBCT gives a higher effective dose than CT (a factor 1.3-4.5), when the same scan range is used. For the lower radiation dose CBCT protocols, the effective dose between CBCT and CT becomes more equal. Meanwhile, for the lowest radiation dose CBCT protocols (group 4), the CT gives a higher effective dose. With 2D-3D-fusion a lower DAP is recieved and should be chosen instead of 3D-3D-fusion, considering the radiation dose to the patient. Personnel working in OR that uses CBCT should stand at a long distance from the patient center and placed behind a radiation shield wearing radiation protection aprons. This project will result in a change of the CBCT EVAR protocol names, to receive a better perception of what each protocol entails.

Acknowledgements

I would like to give a special thanks to my supervisors Maria Larsson and Pernilla Jonasson, for guidance and support throughout this work. I would also like to thank Mårten Falkenberg and Per Wessberg for valuable information about EVAR and scoliosis procedures. Lastly, I wish to thank Jimmy Holmström for all your help with the choice of protocols and demonstration of the CBCT modalities and Helen Milde for your help with CT.

Reference list

1. Richter, P.H., et al., *One Year Orthopaedic Trauma Experience Using an Advanced Interdisciplinary Hybrid Operating Room.* Injury, 2015. **46 Suppl 4**: p. S129-134.
2. Miller, D.L. and R. Society for Interventional, *Interventional Fluoroscopy: Reducing Radiation Risks for Patients and Staff.* J Vasc Interv Radiol, 2009. **20**(7 Suppl): p. S274.
3. Tuominen, P. *Ballongvidgning av Kranskärl*. 2017 2017-03-27 2018-09-10]; Available from: https://www.1177.se/Stockholm/Fakta-och-rad/Behandlingar/Ballongvidgning-av-kranskarl-/.
4. Tuominen, P. *Angiografi*. 2017 2017-04-20 2018-09-10]; Available from: https://www.1177.se/Stockholm/Fakta-och-rad/Undersokningar/Angiografi/.
5. Svalkvist, A., J. Hansson, and M. Bath, *Estimating Effective Dose from 3D Imaging with Interventional Fluoroscopy Systems Using Limited Exposure Data.* Acta Radiol, 2016. **57**(3): p. 356-361.
6. Dance, D.R., et al., *Diagnostic Radiology Physics A Handbook for Teachers and Students*. 2014, International Atomic Energy Agency: Vienna, Austria.
7. Krishnaswamy, A., E.M. Tuzcu, and S.R. Kapadia, *Three-dimensional Computed Tomography in the Cardiac Catheterization Laboratory.* Catheter Cardiovasc Interv, 2011. **77**(6): p. 860-865.
8. England, A. and R. Mc Williams, *Endovascular Aortic Aneurysm Repair (EVAR).* Ulster Med J, 2013. **82**(1): p. 3-10.
9. Koutouzi, G., *Three-dimensional Guidance for Endovascular Aortic Repair*. 2017: Department of Radiolody, Institute of Clinical Sciences, Sahlgrenska Academy at University of Gothenburg.
10. Bunnell, W.P., *The Natural History of Idiopathic Scoliosis Before Skeletal Maturity.* Spine (Phila Pa 1976), 1986. **11**(8): p. 773-776.
11. Abul-Kasim, K., et al., *Low-dose Helical Computed Tomography (CT) in the Perioperative Workup of Adolescent Idiopathic Scoliosis.* Eur Radiol, 2009. **19**(3): p. 610-618.
12. Yaman, O. and S. Dalbayrak, *Idiopathic Scoliosis.* Turk Neurosurg, 2014. **24**(5): p. 646-657.
13. Burnei, G., et al., *Congenital Scoliosis: An up-to-date.* J Med Life, 2015. **8**(3): p. 388-397.
14. Hsieh, J., *Computed Tomography: Principles, Design, Artifacts, and Recent Advances*. Third edition ed. 2015, Washington, USA: Society of Photo-Optical Instrumentation Engineers
15. Boone, J.M., *The Trouble With CTD100.* Med Phys, 2007. **34**(4): p. 1364-1371.
16. Mori, S., et al., *Enlarged Longitudinal Dose Profiles in Cone-beam CT and the Need for Modified Dosimetry.* Med Phys, 2005. **32**(4): p. 1061-1069.
17. Lechuga, L. and G.A. Weidlich, *Cone Beam CT vs. Fan Beam CT: A Comparison of Image Quality and Dose Delivered Between Two Differing CT Imaging Modalities.* Cureus, 2016. **8**(9): p. e778.
18. Surendran, S., et al., *Use of 3-D Digital Subtraction Rotational Angiography During Cardiac Catheterization of Infants and Adults with Congenital Heart Diseases.* Catheterization and Cardiovascular Interventions, 2017. **90**(4): p. 618-625.
19. van Rooij, W.J., et al., *3D Rotational Angiography: The New Gold Standard in the Detection of Additional Intracranial Aneurysms.* American Journal of Neuroradiology, 2008. **29**(5): p. 976-979.
20. Tonkopi, E., A.H. Al-Habsi, and J.J. Shankar, *Radiation Dose from 3D Rotational vs. Conventional 2D Digital Subtraction Angiography in Intracranial Aneurysm Coiling.* Can J Neurol Sci, 2015. **42**(3): p. 176-180.
21. Mitrovic, U., et al., *Simultaneous 3D-2D Image Registration and C-arm Calibration: Application to Endovascular Image-guided Interventions.* Med Phys, 2015. **42**(11): p. 6433-6447.
22. Mitrovic, U., et al., *3D-2D Registration in Endovascular Image-guided Surgery: Evaluation of State-of-the-art Methods on Cerebral Angiograms.* Int J Comput Assist Radiol Surg, 2018. **13**(2): p. 193-202.

23. Bushong, S.C., *Radiologic Science for Technologists: Physics, Biology, and Protection*. 9th edition ed. 2008, St. Louis, Missouri: Mosby Elsevier.
24. Isaksson, M., *Grundläggande Strålningsfysik*. 2011, Studentlitteratur AB: Lund. p. 130-131.
25. Thermo Fisher Scientific, *Thermo Scientific Harshaw TLD Materials and Dosimeters*, T.F. Scientific, Editor. 2016, Thermo Fisher Scientific
26. ICRP, *The 2007 Recommendations of the International Commission on Radiological Protection. ICRP Publication 103. Ann. ICRP 37 (2-4)*. 2007.
27. Tapiovaara, M. and T. Siiskonen, *PCXMC, A PC-based Monte Carlo Program for Calculating Patient Doses in Medical X-ray Examinations (2nd Ed.) STUK-A231*. 2008, Finnish Centre for Radiation and Nuclear Safety: Helsinki.
28. Tapiovaara, M., *PCXMC 2.0 Supplementary Programs User´s Guide*. 2012, Finnish Centre for Radiation and Nuclear Safety: Helsinki.
29. ICRP, *1990 Recommendations of the International Commission on Radiological Protection. ICRP Publication 60. Ann. ICRP 21 (1-3).* 1991.
30. Stamm, G. and H.D. Nagel, *CT-Expo v2.5 A Tool for Dose Evaluation in Computed Tomography User's guide*. 2017.
31. Laboratory, T.P., *Catphan 500 and 600 Manual*. 2004, The Phantom Laboratory.
32. Agency, I.A.E., *Dosimetry in Diagnostic Radiology: An International Code of Practice, Technical Reports Series No. 457*. 2007, International Atomic Energy Agency: Vienna, Austria. p. 73-75.
33. Grimbergen, T.W.M., et al., *Dosimetry of Low and Medium Energy X-rays: A Code of Practice for Use in Radiotherapy and Radiobiology*. 1997, Netherlands Commission on Radiation Dosimetry.
34. Healthineers, S. *Simulation of X-ray Spectra Online tool for the simulation of X-ray Spectra*. 2018 [cited 2018 15-11-2018]; Available from: https://www.oem-xray-components.siemens.com/x-ray-spectra-simulation.
35. Amato, E., et al., *Can Contrast Media Increase Organ Doses in CT Examinations? A Clinical Study.* AJR Am J Roentgenol, 2013. **200**(6): p. 1288-1293.

Appendix A – Protocol settings

In Table A.1, A.2 and A.3, the protocols settings are presented for each of the modalities, *Artis Q*, *Pheno* and *Zeego*.

Table A.1: Exposure and image settings for the protocols on Artis Q.

	Protocols on Artis Q			
Setting	**6sDCT Body**	**5sDCT Body Care**	**5sDR Body**	**5sDR Body Care**
X-ray tube voltage (kV)	90	90	90	90
Pulse width (ms)	5.0	5.0	12.5	12.5
Dose (µGy/f)	0.36	0.36	0.36	0.10
Min Cu filter (mmCu)	0	0	0	0.1
Max Cu filter (mmCu)	0	0	0	0.1
Resolution	Low	Low	Medium	Medium
3D Angle Step (°/f)	0.50	0.80	1.50	1.50
Number of projections	395	247	132	132

Table A.2: Exposure and image settings for the protocols on Artis Pheno.

	Protocols on Artis Pheno					
Setting	**5sDCT Body L**	**4sDCT Body Care L**	**4sDR Body L**	**4sDR Body Care**	**4sRygg Normal dose 3D**	**4sRygg Low dose 3D**
X-ray tube voltage (kV)	90	90	90	90	125	125
Pulse width (ms)	8.0	8.0	8.0	8.0	8.0	8.0
Dose (µGy/f)	0.36	0.36	0.36	0.10	0.10	0.080
Min Cu filter (mmCu)	0	0	0	0.1	0.1	0.1
Max Cu filter (mmCu)	0	0	0	0.1	0.1	0.1
Resolution	Low	Low	Medium	Medium	Medium	Medium
3D Angle Step (°/f)	0.50	0.80	1.50	1.50	1.50	1.50
Number of projections	397	248	133	133	133	133

Table A.3: Exposure and image settings for the protocols on Artis Zeego.

	Protocols on Artis Zeego					
Setting	**8sDCT Body R30**	**5sDCT Body Care R30**	**5sDR Body R30**	**5sDR Body Care R30**	**CT Normal dose 5s R15P85**	**CT Low dose 4s R15P85**
X-ray tube voltage (kV)	90	90	90	90	125	125
Pulse width (ms)	5.0	5.0	12.5	12.5	12.5	12.5
Dose (µGy/f)	0.36	0.36	0.36	0.10	0.10	0.10
Min Cu filter (mmCu)	0	0	0	0.1	0.1	0.1
Max Cu filter (mmCu)	0	0	0	0.1	0.9	0.9
Resolution	Low	Low	Medium	Medium	Medium	Medium
3D Angle Step (°/f)	0.50	0.80	1.50	1.50	1.50	3.0
Number of projections	397	248	133	133	133	67

Appendix B – Abdominal phantom radiation doses

In Table B.1-B.3 the radiation dose data for all CBCT EVAR protocols, with different settings, on *Artis Q*, *Pheno* and *Zeego* are presented.

Table B.1: DAP [$Gycm^2$], DAP/A [mGy], $D_{skin,DICOM}$ [mGy], $\dot{D}$ [mGy/s], with an uncertainty of ±10%, E [mSv], $D_{skin,PCXMC}$, D_{ABM}, D_{colon}, $D_{kidneys}$, $D_{ovaries}$ and D_{SI} [mGy] for each EVAR protocol and setting on Artis Q, for one CBCT, using the abdominal phantom.

Radiation dose quantities for the protocols on Artis Q

Protocol	Setting	DAP [$Gycm^2$]	DAP/ A [mGy]	$D_{skin, DICOM}$ [mGy]	$\dot{D}$ [mGy/s]	E [mSv]	$D_{skin, PCXMC}$ [mGy]	D_{ABM} [mGy]	D_{colon} [mGy]	$D_{kidneys}$ [mGy]	$D_{ovaries}$ [mGy]	D_{SI} [mGy]
6sDCT Body	Default	55	46	180	30	4.9±27%	5.6±18%	10±13%	13±32%	12±49%	16±176%	17±22%
	Col 1	46	52	210	36	4.3±27%	4.8±18%	10±12%	13±31%	5.0±63%	15±172%	17±20%
	Col 2	28	57	240	41	2.9±22%	3.1±18%	7.6±11%	8.9±30%	2.1±71%	7.3±178%	14±18%
	Zoom 42	48	71	210	36	3.9±26%	3.2±19%	9.0±11%	11±30%	6.3±51%	14±152%	15±19%
	Zoom 32	38	170	280	48	2.0±21%	1.3±20%	5.3±9.5%	5.8±29%	1.6±59%	6.6±145%	11±15%
5sDCT Body Care	Default	35	28	110	26	3.1±21%	3.5±14%	6.5±10%	8.3±26%	7.6±39%	10±138%	11±17%
	Col 1	29	33	130	31	2.7±21%	3.1±14%	6.5±9.8%	8.1±25%	3.2±49%	9.3±137%	11±16%
	Col 2	18	37	150	36	1.8±18%	2.0±14%	4.9±9.1%	5.6±24%	1.3±57%	4.7±143%	8.8±14%
	Zoom 42	31	45	130	31	2.5±20%	2.0±15%	5.7±8.8%	6.9±24%	4.0±40%	9.1±119%	9.6±15%
	Zoom 32	24	110	180	43	1.3±17%	0.83±16%	3.4±7.6%	3.7±23%	1.0±46%	4.2±114%	7.2±12%
5sDR Body	Default	19	16	61	12	1.7±16%	1.9±10%	3.6±7.6%	4.6±19%	4.1±28%	5.5±103%	5.8±12%
	Col 1	18	20	72	14	1.5±16%	1.6±10%	3.5±7.2%	4.3±18%	1.6±37%	5.0±102%	5.8±12%
	Col 2	11	22	91	17	1.0±13%	1.1±10%	2.6±6.8%	3.0±17%	0.68±44%	2.4±109%	4.8±11%
	Zoom 42	17	25	72	14	1.4±15%	1.1±11%	3.1±6.4%	3.8±17%	2.2±29%	5.0±88%	5.3±11%
	Zoom 32	17	76	130	24	0.78±13%	0.55±12%	2.0±5.9%	2.3±17%	0.59±37%	2.5±89%	4.3±9.3%
5sDR Body Care	Default	3.5	2.9	11	2.2	0.40±16%	0.36±11%	0.83±7.7%	1.1±19%	0.93±28%	1.4±101%	1.4±12%
	Col 1	3.0	3.4	14	2.6	0.36±16%	0.31±11%	0.80±7.3%	1.1±17%	0.38±37%	1.3±99%	1.4±11%
	Col 2	2.0	4.1	17	3.3	0.24±13%	0.21±11%	0.62±7.0%	0.76±17%	0.17±44%	0.62±106%	1.2±11%
	Zoom 42	3.2	4.6	13	2.6	0.28±15%	0.18±12%	0.62±6.6%	0.79±17%	0.43±29%	1.1±87%	1.1±11%
	Zoom 32	3.2	14	24	4.5	0.20±13%	0.11±13%	0.48±6.1%	0.58±17%	0.15±36%	0.65±88%	1.1±9.1%

Table B.2: DAP [Gycm²], DAP/A [mGy], $D_{skin,DICOM}$ [mGy], $\dot{D}$ [mGy/s], with an uncertainty of ±10%, E [mSv], $D_{skin,PCXMC}$, D_{ABM}, D_{colon}, $D_{kidneys}$, $D_{ovaries}$ and D_{SI} [mGy] for each EVAR protocol and setting on Artis Pheno, for one CBCT, using the abdominal phantom.

Radiation dose quantities for the protocols on Artis Pheno

Protocol	Setting	DAP [Gycm²]	DAP/A [mGy]	$D_{skin,DICOM}$ [mGy]	$\dot{D}$ [mGy/s]	E [mSv]	$D_{skin,PCXMC}$ [mGy]	D_{ABM} [mGy]	D_{colon} [mGy]	$D_{kidneys}$ [mGy]	$D_{ovaries}$ [mGy]	D_{SI} [mGy]
5sDCT Body L	Default	55	46	200	40	5.7±25%	5.0±18%	8.9±15%	18±29%	7.9±60%	19±159%	23±19%
	Col 1	47	49	220	44	5.1±26%	4.5±18%	8.6±15%	17±28%	4.4±66%	18±158%	23±17%
	Col 2	32	66	270	55	3.4±22%	3.1±18%	6.6±15%	12±28%	1.9±77%	9.0±167%	20±16%
	Zoom 42	51	80	250	50	4.3±25%	2.9±19%	7.0±15%	14±27%	3.5±63%	17±139%	21±16%
	Zoom 32	50	230	420	86	2.9±20%	1.7±19%	5.6±13%	9.5±25%	1.7±62%	8.8±138%	22±12%
4sDCT Body Care L	Default	35	29	120	32	3.6±20%	3.2±14%	5.6±12%	11±23%	5.0±48%	12±127%	14±15%
	Col 1	30	31	140	35	3.2±30%	2.8±14%	5.4±12%	11±22%	2.8±53%	11±123%	14±14%
	Col 2	18	38	180	45	2.0±17%	1.8±15%	3.9±11%	6.9±22%	1.1±61%	5.0±137%	12±13%
	Zoom 42	32	50	150	40	2.7±20%	1.8±15%	4.4±11%	8.7±22%	2.2±50%	11±111%	13±13%
	Zoom 32	32	150	270	71	1.9±16%	1.1±15%	3.6±10%	6.0±20%	1.1±50%	5.6±111%	14±9.9%
4sDR Body L	Default	18	15	66	17	1.9±15%	1.6±11%	3.0±8.9%	5.9±17%	2.6±35%	6.3±92%	7.6±11%
	Col 1	16	16	72	18	1.7±15%	1.5±10%	2.9±8.8%	5.5±16%	1.4±39%	5.7±92%	7.6±10%
	Col 2	9.2	19	96	25	0.92±12%	0.87±11%	1.9±8.3%	3.2±16%	0.51±45%	2.3±99%	5.8±9.2%
	Zoom 42	17	27	82	21	1.4±15%	0.96±11%	2.4±8.6%	4.6±16%	1.2±36%	5.7±81%	7.0±9.2%
	Zoom 32	18	84	150	39	1.0±11%	0.59±11%	2.0±7.7%	3.3±15%	0.60±37%	3.0±80%	7.4±7.3%
4sDR Body Care	Default	3.7	3.1	13	3.4	0.45±15%	0.32±11%	0.70±9.0%	1.4±16%	0.62±35%	1.5±90%	1.8±11%
	Col 1	3.1	3.3	14	3.7	0.39±15%	0.28±11%	0.67±8.9%	1.3±16%	0.33±38%	1.4±91%	1.8±10%
	Col 2	1.9	3.9	19	4.8	0.22±12%	0.17±11%	0.45±8.5%	0.75±16%	0.13±45%	0.55±98%	1.4±9.1%
	Zoom 42	3.4	5.3	16	4.2	0.34±15%	0.19±12%	0.56±8.6%	1.1±16%	0.29±36%	1.4±79%	1.7±9.0%
	Zoom 32	4.8	23	41	10	0.28±13%	0.15±13%	0.53±8.4%	0.90±16%	0.17±40%	0.84±87%	2.0±7.9%

Table B.3: DAP [Gycm²], DAP/A [mGy], $D_{skin,DICOM}$ [mGy], $\dot{D}$ [mGy/s], with an uncertainty of ±10%, E [mSv], $D_{skin,PCXMC}$, D_{ABM}, D_{colon}, $D_{kidneys}$, $D_{ovaries}$ and D_{SI} [mGy] for each EVAR protocol and setting on Artis Zeego, for one CBCT, using the abdominal phantom.

Radiation dose quantities for the protocols on Artis Zeego

Protocol	Setting	DAP [$Gycm^2$]	DAP/A [mGy]	$D_{skin, DICOM}$ [mGy]	$\dot{D}$ [mGy/s]	E [mSv]	$D_{skin, PCXMC}$ [mGy]	D_{ABM} [mGy]	D_{colon} [mGy]	$D_{kidneys}$ [mGy]	$D_{ovaries}$ [mGy]	D_{SI} [mGy]
8sDCT Body R30	Default	53	45	170	25	5.8±26%	6.4±17%	12±13%	16±31%	14±48%	19±166%	20±21%
	Col 1	41	47	190	27	5.1±25%	5.2±17%	12±12%	15±29%	5.8±58%	18±158%	20±19%
	Col 2	24	51	210	31	3.4±21%	3.2±17%	8.8±11%	11±27%	2.5±64%	9.1±160%	17±16%
	Zoom 42	43	63	180	27	4.4±24%	3.4±18%	10±11%	12±29%	7.1±48%	16±144%	17±18%
5sDCT Body Care R30	Default	34	29	110	20	3.7±21%	4.1±14%	7.9±10%	10±25%	9.2±38%	12±132%	13±16%
	Col 1	26	30	120	22	3.2±20%	3.3±14%	7.6±9.3%	9.7±23%	3.6±46%	11±126%	13±15%
	Col 2	16	32	140	24	2.2±17%	2.1±14%	5.6±8.5%	6.8±22%	1.6±51%	5.7±129%	11±13%
	Zoom 42	28	40	120	21	2.8±19%	2.2±14%	6.5±8.5%	7.9±23%	4.5±38%	11±114%	11±14%
5sDR Body R30	Default	22	18	72	13	2.2±16%	2.6±10%	4.7±7.7%	6.2±19%	5.4±29%	7.3±101%	7.6±13%
	Col 1	19	21	86	15	2.0±16%	2.3±10%	4.6±7.4%	6.0±18%	2.1±36%	6.7±100%	7.8±12%
	Col 2	13	27	110	20	1.3±13%	1.6±11%	3.5±7.1%	4.3±18%	0.93±43%	3.3±108%	6.5±11%
	Zoom 42	19	27	78	14	1.7±15%	1.4±11%	3.9±6.6%	4.9±18%	2.7±30%	6.2±88%	6.6±11%
5sDR Body Care R30	Default	4.3	3.6	14	2.4	0.54±16%	0.50±11%	1.1±7.8%	1.5±18%	1.2±29%	1.8±99%	1.9±12%
	Col 1	3.6	4.1	16	2.9	0.48±16%	0.42±11%	1.1±7.5%	1.5±17%	5.1±36%	1.7±98%	1.9±11%
	Col 2	2.5	5.2	22	3.9	0.32±13%	0.29±11%	0.81±7.0%	1.0±17%	0.22±43%	0.78±107%	1.6±11%
	Zoom 42	3.6	5.3	15	2.7	0.42±15%	0.28±12%	0.93±6.7%	1.2±17%	0.65±30%	1.6±86%	1.7±11%

In Figure B.1a-d the effective dose, for all CBCT EVAR protocols and settings, on *Artis Q*, *Pheno* and *Zeego* are presented. The protocol numbers 1-4 represents the highest to the lowest radiation dose protocol on each modality.

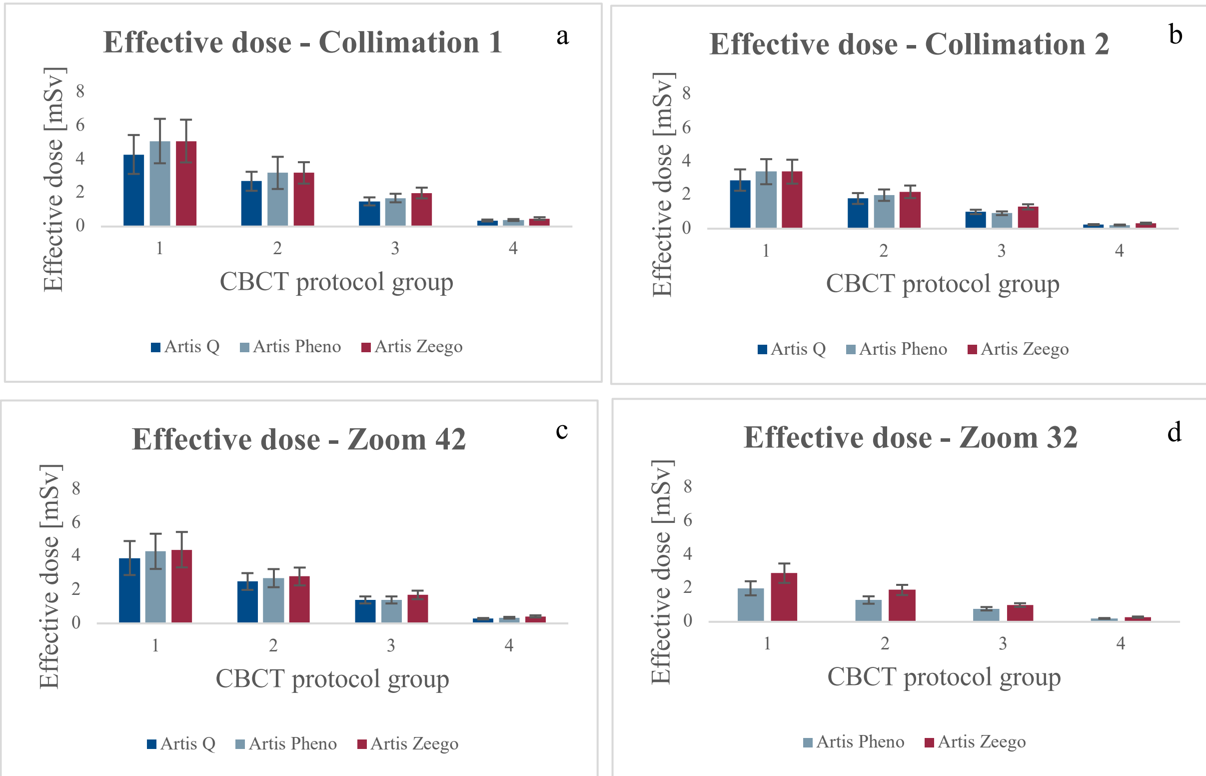

Figure B.1: Effective dose [mSv], using the abdominal phantom and different settings, for all protocols on Artis Q, Artis Pheno and Artis Zeego. The settings used were collimation 1, collimation 2, zoom 42 and zoom 32, presented in figure a, b, c and d, respectively. The protocols 1-4 represents the high to the low radiation dose CBCT protocols. The error bars indicate the uncertainties in calculations with PCXMX20Rotation.

In Table B.4-B.6 the relative difference between the CBCT EVAR protocols on each modality, *Artis Q*, *Pheno* and *Zeego*, are presented. The radiation dose quantities for the three highest radiation dose protocols have been compared to the lowest radiation dose protocol.

*Table B.4: Relative radiation dose values between the protocols on Artis Q compared to the low dose protocol 5sDR Body Care, using the abdominal phantom. *All protocols and radiation dose quantities, using the default setting, are significantly different (p-value<0.05).*

		Relative difference between radiation dose quantities for the protocols on Artis Q									
Protocol	**Setting**	**DAP**	**$D_{skin, DICOM}$**	**$\dot{D}$**	**E**	**$D_{skin, PCXMC}$**	**D_{ABM}**	**D_{colon}**	**$D_{kidneys}$**	**$D_{ovaries}$**	**D_{SI}**
6sDCT Body	Default*	16	16	14	12	15	13	12	13	12	12
	Col 1	15	15	14	12	16	13	12	13	12	12
	Col 2	14	14	13	12	14	12	12	12	12	11
	Zoom 42	16	16	14	14	18	15	14	14	14	14
	Zoom 32	12	12	11	10	12	11	9.9	10	10	10
5sDCT Body Care	Default*	9.8	9.8	12	7.6	9.7	7.9	7.4	8.1	7.3	7.4
	Col 1	9.7	9.7	12	7.7	9.9	8.0	7.5	8.3	7.5	7.5
	Col 2	8.8	8.9	11	7.5	9.2	7.8	7.4	7.5	7.5	7.3
	Zoom 42	9.8	9.8	12	8.8	11	9.2	8.7	9.2	8.6	8.6
	Zoom 32	7.6	7.6	9.6	6.6	7.7	7.0	6.3	6.6	6.5	6.5
5sDR Body	Default*	5.4	5.4	5.4	4.2	5.3	4.3	4.1	4.4	4.0	4.1
	Col 1	5.9	5.3	5.3	4.1	5.3	4.3	4.1	4.2	4.0	4.0
	Col 2	5.3	5.3	5.3	4.0	5.1	4.2	3.9	3.9	3.8	3.9
	Zoom 42	5.4	5.4	5.4	4.8	6.3	5.0	4.8	5.0	4.7	4.7
	Zoom 32	5.4	5.4	5.4	4.0	5.1	4.2	3.9	3.9	3.8	3.9

*Table B.5: Relative radiation dose values between the protocols on Artis Pheno compared to the low dose protocol 4sDR Body Care, using the abdominal phantom. *All protocols and radiation dose quantities, using the default setting, are significantly different (p-value<0.05).*

		Relative difference between radiation dose quantities for the protocols on Artis Pheno									
Protocol	**Setting**	**DAP**	**$D_{skin, DICOM}$**	**$\dot{D}$**	**E**	**$D_{skin, PCXMC}$**	**D_{ABM}**	**D_{colon}**	**$D_{kidneys}$**	**$D_{ovaries}$**	**D_{SI}**
5sDCT Body L	Default*	15	15	12	13	16	13	13	13	12	13
	Col 1	15	15	12	13	16	13	13	13	13	13
	Col 2	17	14	11	16	19	15	16	15	16	15
	Zoom 42	15	15	12	13	16	13	13	12	12	13
	Zoom 32	10	10	8.2	11	11	11	11	10	11	11
4sDCT Body Care L	Default*	9.4	9.4	9.5	8.0	9.9	8.0	8.0	8.0	7.7	8.0
	Col 1	9.5	9.5	9.5	8.2	10	8.1	8.2	8.4	8.0	8.1
	Col 2	9.7	9.4	9.4	9.0	11	8.8	9.2	8.7	9.2	8.8
	Zoom 42	9.5	9.5	9.5	7.9	9.8	7.9	8.0	7.7	7.7	7.9
	Zoom 32	6.7	6.7	6.8	6.7	7.2	6.8	6.7	6.7	6.6	6.8
4sDR Body L	Default*	5.0	5.0	5.0	4.2	5.0	4.2	4.2	4.3	4.1	4.2
	Col 1	5.0	5.0	5.0	4.2	5.2	4.3	4.2	4.2	4.1	4.2
	Col 2	4.9	5.2	5.2	4.2	5.3	4.3	4.2	4.1	4.1	4.2
	Zoom 42	5.0	5.0	5.0	4.2	5.2	4.3	4.2	4.2	4.1	4.2
	Zoom 32	3.7	3.7	3.7	3.6	4.0	3.7	4.0	3.6	3.6	3.7

Table B.6: Relative radiation dose values between the protocols on Artis Zeego compared to the low dose protocol 5sDR Body Care R30, using the abdominal phantom.

		Relative difference between radiation dose quantities for the protocols on Artis Zeego									
Protocol	**Setting**	**DAP**	$D_{skin, DICOM}$	$\dot{D}$	**E**	$D_{skin, PCXMC}$	D_{ABM}	D_{colon}	$D_{kidneys}$	$D_{ovaries}$	D_{SI}
8sDCT Body R30	Default	13	13	10	11	13	11	10	12	11	11
	Col 1	11	11	9.4	11	12	11	10	11	10	10
	Col 2	9.7	9.6	7.9	11	11	11	10	11	12	10
	Zoom 42	12	12	9.8	10	12	11	10	11	10	10
5sDCT Body Care R30	Default	8.0	8.0	8.1	6.9	8.3	7.2	6.7	7.4	6.8	6.8
	Col 1	7.2	7.3	7.3	6.7	7.8	7.0	6.5	7.0	6.6	6.6
	Col 2	6.2	6.2	6.2	6.9	7.2	7.0	6.6	7.2	7.3	6.6
	Zoom 42	7.7	7.7	7.7	6.7	8.0	7.1	6.5	7.0	6.6	6.6
5sDR Body R30	Default	5.2	5.2	5.2	4.1	5.3	4.2	4.0	4.3	4.0	4.0
	Col 1	5.2	5.2	5.2	4.1	5.3	4.2	4.0	4.1	4.0	4.0
	Col 2	5.2	5.2	5.2	4.3	5.5	4.4	4.2	4.2	4.2	4.1
	Zoom 42	5.1	5.1	5.1	4.0	5.3	4.2	4.0	4.2	3.9	4.0

Table B.7-B.10 presents the percentage difference in radiation dose for the same protocols on the different modalities, *Artis Q*, *Pheno* and *Zeego*.

Table B.7: Percentage change in radiation dose for the same protocols on different modalities, using the abdominal phantom. The protocols 5sDCT Body L on Artis Pheno and 8sDCT Body R30 on Artis Zeego was compared to 6sDCT Body on Artis Q.

			Percentage radiation dose change for the same protocol on different modalities									
Modality	**Protocol**	**Setting**	**DAP [%]**	**$D_{skin, DICOM}$ [%]**	**$\dot{D}$ [%]**	**E [%]**	**$D_{skin, PCXMC}$ [%]**	**D_{ABM} [%]**	**D_{colon} [%]**	**$D_{kidneys}$ [%]**	**$D_{ovaries}$ [%]**	**D_{SI} [%]**
Artis Pheno	5sDCT Body L	Default	0.5	12	32	17	-10	-14	34	-34	19	37
		Col 1	3.5	4.2	24	18	-7.2	-16	34	-11	21	36
		Col 2	15	12	33	18	0.51	-14	36	-6.5	23	44
		Zoom 42	3.6	19	41	11	-11	-22	28	-44	18	39
		Zoom 32	31	50	78	45	20	5.6	64	11	34	93
Artis Zeego	8sDCT Body R30	Default	-2.3	-2.7	-17	20	14	20	21	19	22	21
		Col 1	-10	-10	-23	18	6.5	16	19	17	20	18
		Col 2	-12	-12	-25	20	5.1	16	22	21	24	20
		Zoom 42	-12	-13	-26	13	5.5	13	14	13	25	14

Table B.8: Percentage change in radiation dose for the same protocols on different modalities, using the abdominal phantom. The protocols 4sDCT Body Care L on Artis Pheno and 5sDCT Body Care R30 on Artis Zeego was compared to 5sDCT Body Care on Artis Q.

			Percentage radiation dose change for the same protocol on different modalities									
Modality	**Protocol**	**Setting**	**DAP [%]**	**$D_{skin, DICOM}$ [%]**	**$\dot{D}$ [%]**	**E [%]**	**$D_{skin, PCXMC}$ [%]**	**D_{ABM} [%]**	**D_{colon} [%]**	**$D_{kidneys}$ [%]**	**$D_{ovaries}$ [%]**	**D_{SI} [%]**
Artis Pheno	4sDCT Body Care L	Default	1.1	12	21	17	-9.7	-14	34	-34	18	37
		Col 1	2.0	3.3	13	17	-7.9	-16	32	-12	19	34
		Col 2	4.1	15	24	7.7	-7.0	-19	23	-17	8.3	36
		Zoom 42	2.9	18	27	10	-11	-22	27	-45	17	38
		Zoom 32	33	52	65	45	30	6.4	64	11	32	92
Artis Zeego	5sDCT Body Care R30	Default	0.58	0.13	-25	22	17	22	24	21	24	23
		Col 1	-9.5	-8.2	-30	18	7.5	17	20	14	29	29
		Col 2	-11	-11	-33	19	5.5	16	22	20	22	20
		Zoom 42	-10	-11	-33	15	7.7	14	15	14	16	15

Table B.9: Percentage change in radiation dose for the same protocols on different modalities, using the abdominal phantom. The protocols 4sDR Body L on Artis Pheno and 5sDR Body R30 on Artis Zeego was compared to 5sR Body on Artis Q.

			Percentage radiation dose change for the same protocol on different modalities									
Modality	**Protocol**	**Setting**	**DAP [%]**	**$D_{skin, DICOM}$ [%]**	**$\dot{D}$ [%]**	**E [%]**	**$D_{skin, PCXMC}$ [%]**	**D_{ABM} [%]**	**D_{colon} [%]**	**$D_{kidneys}$ [%]**	**$D_{ovaries}$ [%]**	**D_{SI} [%]**
Artis Pheno	4sDR Body L	Default	-2.3	8.6	47	12	-16	-17	28	-36	14	32
		Col 1	-11	-0.40	35	13	-10	-17	27	-13	14	30
		Col 2	-13	4.9	42	-4.9	-21	-26	6.3	-25	-5.8	22
		Zoom 42	-0.69	14	54	6.7	-14	-22	21	-45	14	33
		Zoom 32	4.5	20	62	30	7.3	-2.1	43	2.0	21	73
Artis Zeego	5sDR Body R30	Default	18	18	11	33	37	30	36	31	32	32
		Col 1	6.8	19	11	34	38	32	39	31	34	34
		Col 2	24	24	16	39	43	35	45	36	38	37
		Zoom 42	9.2	8.4	1.5	26	30	25	28	25	26	25

Table B.10: Percentage change in radiation dose for the same protocols on different modalities, using the abdominal phantom. The protocols 4sDR Body Care L on Artis Pheno and 5sDR Body Care R30 on Artis Zeego was compared to 5sR Body Care on Artis Q.

			Percentage radiation dose change for the same protocol on different modalities									
Modality	**Protocol**	**Setting**	**DAP [%]**	**$D_{skin, DICOM}$ [%]**	**$\dot{D}$ [%]**	**E [%]**	**$D_{skin, PCXMC}$ [%]**	**D_{ABM} [%]**	**D_{colon} [%]**	**$D_{kidneys}$ [%]**	**$D_{ovaries}$ [%]**	**D_{SI} [%]**
Artis Pheno	4sDR Body Care L	Default	4.5	16	57	11	-12	-15	24	-33	12	28
		Col 1	4.5	5.8	43	10	-9.5	-17	22	-13	11	25
		Col 2	-5.0	8.6	47	-9.9	-23	-28	-1.2	-28	-12	13
		Zoom 42	5.9	21	64	23	3.9	-9.5	39	-34	31	51
		Zoom 32	50	73	130	41	39	9.8	55	9.1	29	83
Artis Zeego	5sDR Body Care R30	Default	22	22	14	34	37	33	38	33	35	34
		Col 1	21	22	14	35	38	33	39	34	35	35
		Col 2	26	28	20	31	34	30	36	26	26	32
		Zoom 42	14	13	6.1	51	54	49	55	50	52	50

Table B.11 presents the radiation dose quantities received from the CT EVAR protocols, for different settings.

*Table B.11: $CTDI_{vol}$ [mGy], DLP [mGycm] with an uncertainty of ±10%, E [mSv], H_{skin}, $H_{bone\ marrow}$, $H_{kidneys}$ and $H_{small\ intestine}$ [mSv] with an uncertainty of ±20%, for each CT protocol with the different scan settings, using the abdominal phantom. * CBCT scan range has been used. Fictitious patient (abdominal phantom) personal identity number: 20181105-D062.*

CT protocol	Setting	$CTDI_{vol}$ [mGy]	DLP [mGycm]	E [mSv]	H_{skin} [mSv]	$H_{bone\ marrow}$ [mSv]	$H_{kidneys}$ [mSv]	$H_{small\ intestine}$ [mSv]
Aorta before EVAR	120 kV	5.6	210	3.2	2.7	3.2	6.9	7.5
	100 kV	6.0	230	3.4	2.8	3.4	7.3	7.9
	*120 kV	5.6	130	1.8	1.7	2.4	0.20	3.7
	*100 kV	6.0	140	1.9	1.8	2.9	0.30	3.9
EVAR w/o c + abd. aorta after EVAR	120 kV	11	430	6.4	5.4	6.4	14	15
	100 kV	12	450	6.8	5.6	6.8	15	16
	*120 kV	11	270	3.6	3.4	4.8	0.40	7.4
	*100 kV	12	280	3.8	3.6	5.9	0.60	7.8
Late series EVAR	120 kV	4.2	72	1.0	0.90	0.90	0	0.60
	100 kV	3.9	66	0.90	0.90	0.80	0	0.50
	*120 kV	4.2	110	1.4	1.3	1.9	0.20	3.0
	*100 kV	3.9	97	1.3	1.2	1.7	0.20	2.8

Table B.12 and B.13 shows the radiation dose data for all CBCT scoliosis protocols on *Artis Pheno* and *Artis Zeego*.

Table B.12: DAP [Gycm²], DAP/A [mGy], $D_{skin,DICOM}$ [mGy], $\dot{D}$ [mGy/s], E [mSv], $D_{skin,PCXMC}$, D_{ABM}, D_{colon}, $D_{kidneys}$, $D_{ovaries}$ and D_{SI} [mGy] for each scoliosis protocol and setting on Artis Pheno, for one CBCT, using the abdominal phantom.

		Radiation dose quantities for the protocols on Artis Pheno										
Protocol	**Setting**	**DAP [Gycm²]**	**DAP/A [mGy]**	**$D_{skin, DICOM}$ [mGy]**	**$\dot{D}$ [mGy/s]**	**E [mSv]**	**$D_{skin, PCXMC}$ [mGy]**	**D_{ABM} [mGy]**	**D_{colon} [mGy]**	**$D_{kidneys}$ [mGy]**	**$D_{ovaries}$ [mGy]**	**D_{SI} [mGy]**
5sRygg Normal 3D	Default	2.5	2.1	9.1	2.3	0.33±12%	0.18±10%	0.62±6.1%	0.84±14%	1.0±19%	1.1±76%	1.1±9.5%
5sRygg Low dose 3D	Default	2.1	1.8	7.5	1.9	0.25±12%	0.14±10%	0.47±6.1%	0.64±14%	0.78±19%	0.84±76%	0.82±9.5%

Table B.13: DAP [Gycm²], DAP/A [mGy], $D_{skin,DICOM}$ [mGy], $\dot{D}$ [mGy/s], E [mSv], $D_{skin,PCXMC}$, D_{ABM}, D_{colon}, $D_{kidneys}$, $D_{ovaries}$ and D_{SI} [mGy] for each scoliosis protocol and setting on Artis Zeego, for one CBCT, using the abdominal phantom.

		Radiation dose quantities for the protocols on Artis Zeego										
Protocol	**Setting**	**DAP [Gycm²]**	**DAP/A [mGy]**	**$D_{skin, DICOM}$ [mGy]**	**$\dot{D}$ [mGy/s]**	**E [mSv]**	**$D_{skin, PCXMC}$ [mGy]**	**D_{ABM} [mGy]**	**D_{colon} [mGy]**	**$D_{kidneys}$ [mGy]**	**$D_{ovaries}$ [mGy]**	**D_{SI} [mGy]**
CT Normal dose 5s R15P85	Default	1.8	1.5	5.7	1.1	0.43±15%	0.21±14%	0.74±8.1 %	1.0±18%	1.4±23%	1.3±95%	1.3±12%
CT Low dose 4s R15P85*	Default	0.98	0.81	3.1	0.7	0.24±11%	0.11±9.7	0.41±5.7 %	0.58±13%	0.77±16%	0.74±68%	0.73±8.6 %

In Table B.14 the relative difference between the CBCT scoliosis protocols on each modality, *Artis Pheno* and *Artis Zeego*, are presented. The radiation dose quantities for the highest radiation dose protocol have been compared to the lowest radiation dose protocol.

Table B.14: Relative radiation dose values, using the abdominal phantom, between the protocols 5sRygg Normal dose 3D and CT Normal dose 5s R15P8 compared with 5sRygg Low dose 3D and CT Low dose 4s R15P85, respectively. * Note that CT Low dose 4s R15P85 uses the 3D angle step 3.0°/f instead of 1.5°/f.*

Protocol	Setting	Relative difference between radiation dose quantities for the protocols on Artis Pheno & Artis Zeego									
		DAP	$D_{skin, DICOM}$	$\dot{D}$	E	$D_{skin, PCXMC}$	D_{ABM}	D_{colon}	$D_{kidneys}$	$D_{ovaries}$	D_{SI}
5sRygg Normal 3D	Default	1.2	1.2	1.2	1.3	1.3	1.3	1.3	1.3	1.3	1.3
CT Normal dose 5s R15P85	Default	1.8	1.8	1.5	1.8	1.8	1.8	1.8	1.8	1.8	1.8

In Table B.15 the relative difference between the modalities *Artis Pheno* and *Artis Zeego* for the CBCT scoliosis protocols are presented. The radiation dose quantities for the CBCT scoliosis protocols on *Artis Pheno* has been compared to the scoliosis protocols on *Artis Zeego*.

Table B.15: Percentage difference in radiation dose, using the abdominal phantom, between 5sRygg Normal dose 3D and 5sRygg Low dose 3D on Artis Pheno with CT Normal dose 5s R15P85 and CT Low dose 4s R15P85 on Artis Zeego, respectively. * Note that CT Low dose 4s R15P85 uses the 3D angle step 3.0°/f instead of 1.5°/f.*

Protocol	Setting	Percentage difference in radiation dose for the same protocol on different modalities									
		DAP [%]	$D_{skin,DICOM}$ [%]	$\dot{D}$ [%]	E [%]	$D_{skin,PCXMC}$ [%]	D_{ABM} [%]	D_{colon} [%]	$D_{kidneys}$ [%]	$D_{ovaries}$ [%]	D_{SI} [%]
5sRygg Normal dose 3D	Default	43	60	120	-23	-13	-16	-20	-27	-17	-18
5sRygg Low dose 3D	Default	120	140	170	5.8	20	15	11	1.0	14	12

Table B.16 presents the radiation dose quantities received from the CT scoliosis protocols, for different settings.

*Table B.16: $CTDI_{vol}$ [mGy], DLP [mGycm] with an uncertainty of ±10%, E [mSv], H_{skin}, $H_{bone\ marrow}$, $H_{kidneys}$ and $H_{small\ intestine}$ [mSv] with an uncertainty of ±20%, for each CT protocol with the different scan settings, using the abdominal phantom. * CBCT scan range has been used. Fictitious patient (abdominal phantom) personal identity number: 20181105-D062.*

CT protocol	Setting	$CTDI_{vol}$ [mGy]	DLP [mGycm]	E [mSv]	H_{skin} [mSv]	$H_{bone\ marrow}$ [mSv]	$H_{kidneys}$ [mSv]	$H_{small\ intestine}$ [mSv]
Full back	Default	0.6	22	0.3	0.3	0.3	0.7	0.8
	Automatic	0.7	28	0.4	0.3	0.4	0.9	0.9
	*Default	0.6	17	0.2	0.2	0.3	0.1	0.6
	*Automatic	0.7	22	0.3	0.3	0.4	0.2	0.8

Appendix C – Personnel radiation doses

Table C.1-C4, C.5-C.8 and C.9-C.11 presents the percentage difference in estimated radiation dose to personnel, when different settings are used compared to the default setting, on each modality *Artis Q*, *Pheno* and *Zeego*, respectively.

Table C.1: Percentage difference in radiation dose to a personnel position when using the default settings and collimation 1 on Artis Q, at different distances from the center of the patient.

	Difference in radiation dose [%] to personnel between the default settings and collimation 1 on Artis Q			
	Protocol			
Distance [cm]	**6sDCT Body**	**5sDCT Body Care**	**5sDR Body**	**5sDR Body Care**
80	-12	-3	-12	-10
150	-12	-14	-14	-15
190	-11	-7	-13	-21
270	-14	-24	-17	-23
310	-21	-12	-8	-10

Table C.2: Percentage difference in radiation dose to a personnel position when using the default settings and collimation 2 on Artis Q, at different distances from the center of the patient.

	Difference in radiation dose [%] to personnel between the default settings and collimation 2 on Artis Q			
	Protocol			
Distance [cm]	**6sDCT Body**	**5sDCT Body Care**	**5sDR Body**	**5sDR Body Care**
80	-29	-27	-28	-39
150	-43	-42	-38	-44
190	-46	-40	-38	-45
270	-50	-52	-43	-46
310	-46	-44	-46	-40

Table C.3: Percentage difference in radiation dose to a personnel position when using the default settings and zoom 42 on Artis Q, at different distances from the center of the patient.

	Difference in radiation dose [%] to personnel between the default settings and zoom 42 on Artis Q			
	Protocol			
Distance [cm]	**6sDCT Body**	**5sDCT Body Care**	**5sDR Body**	**5sDR Body Care**
80	-1	-7	-7	-9
150	-8	-7	-6	-11
190	-9	-12	-6	-10
270	-12	-14	-7	-15
310	-6	-2	-19	0

Table C.4: Percentage difference in radiation dose to a personnel position when using the default settings and zoom 32 on Artis Q, at different distances from the center of the patient.

	Difference in radiation dose [%] to personnel between the default settings and zoom 32 on Artis Q			
	Protocol			
Distance [cm]	**6sDCT Body**	**5sDCT Body Care**	**5sDR Body**	**5sDR Body Care**
80	-6	-3	11	-15
150	-20	-19	-2	-13
190	-23	-25	1	-14
270	-27	-31	-4	-15
310	-23	-22	-16	-20

Table C.5: Percentage difference in radiation dose to a personnel position when using the default settings and collimation 1 on Artis Pheno, at different distances from the center of the patient. For the distance 190 cm the Dose Aware dosimeter had fallen on the floor and the value was invalid.

	Difference in radiation dose [%] to personnel between the default settings and collimation 1 on Artis Pheno			
	Protocol			
Distance [cm]	**5sDCT Body L**	**4sDCT Body Care L**	**4sDR Body L**	**4sDR Body Care**
80	-11	-16	-8	-24
150	-23	-23	-24	-30
190	-	-	-	-
270	-72	-69	-76	-67
310	-66	-60	-56	-57

Table C.6: Percentage difference in radiation dose to a personnel position when using the default settings and collimation 2 on Artis Pheno, at different distances from the center of the patient. For the distance 190 cm the Dose Aware dosimeter had fallen on the floor and the value was invalid.

	Difference in radiation dose [%] to personnel between the default settings and collimation 2 on Artis Pheno			
	Protocol			
Distance [cm]	**5sDCT Body L**	**4sDCT Body Care L**	**4sDR Body L**	**4sDR Body Care**
80	-29	-33	-34	-50
150	-47	-50	-52	-57
190	-	-	-	-
270	-81	-85	-87	-83
310	-77	-78	-72	-71

Table C.7: Percentage difference in radiation dose to a personnel position when using the default settings and zoon 42 on Artis Pheno, at different distances from the center of the patient. For the distance 190 cm the Dose Aware dosimeter had fallen on the floor and the value was invalid.

	Difference in radiation dose [%] to personnel between the default settings and zoom 42 on Artis Pheno			
	Protocol			
Distance [cm]	**5sDCT Body L**	**4sDCT Body Care L**	**4sDR Body L**	**4sDR Body Care**
80	3	-6	-7	-17
150	-15	-17	-18	-23
190	-	-	-	-
270	-70	-73	-71	-67
310	-64	-65	-52	-57

Table C.8: Percentage difference in radiation dose to a personnel position when using the default settings and zoom 32 on Artis Pheno, at different distances from the center of the patient. For the distance 190 cm the Dose Aware dosimeter had fallen on the floor and the value was invalid.

	Difference in radiation dose [%] to personnel between the default settings and zoom 32 on Artis Pheno			
	Protocol			
Distance [cm]	**5sDCT Body L**	**4sDCT Body Care L**	**4sDR Body L**	**4sDR Body Care**
80	27	21	34	15
150	-5	-3	-1	3
190	-	-	-	-
270	-68	-63	-69	-67
310	-57	-51	-44	-43

Table C.9: Percentage difference in radiation dose to a personnel position when using the default settings and collimation 1 on Artis Zeego, at different distances from the center of the patient.

	Difference in radiation dose [%] to personnel between the default settings and collimation 1 on Artis Zeego			
	Protocol			
Distance [cm]	**8sDCT Body R30**	**5sDCT Body Care R30**	**5sDR Body R30**	**5sDR Body Care R30**
80	-15	-16	3	-17
150	-21	-22	-14	-22
190	-22	-24	-20	-38
270	-23	-27	-24	-38
310	-26	-29	-6	-18

Table C.10: Percentage difference in radiation dose to a personnel position when using the default settings and collimation 2 on Artis Zeego, at different distances from the center of the patient.

	Difference in radiation dose [%] to personnel between the default settings and collimation 2 on Artis Zeego			
	Protocol			
Distance [cm]	**8sDCT Body R30**	**5sDCT Body Care R30**	**5sDR Body R30**	**5sDR Body Care R30**
80	-37	-37	-20	-39
150	-51	-49	-37	-47
190	-54	-51	-40	-55
270	-50	-53	-45	-57
310	-63	-57	-46	-55

Table C.11: Percentage difference in radiation dose to a personnel position when using the default settings and zoom 42 on Artis Zeego, at different distances from the center of the patient.

	Difference in radiation dose [%] to personnel between the default settings and zoom 42 on Artis Zeego			
	Protocol			
Distance [cm]	**8sDCT Body R30**	**5sDCT Body Care R30**	**5sDR Body R30**	**5sDR Body Care R30**
80	-12	-13	-11	-23
150	-17	-17	-16	-19
190	-18	-19	-18	-26
270	-18	-23	-24	-33
310	-16	-64	-31	-36